Future trends of accelerator-based light source development

Mau-Sen Chiu
2026/01/09
Beam Dynamics Group, NSRRC

Accelerator-based Light Sources driven by Scientific Applications

Ultra-small & Ultra-fast capabilities enabled by modern accelerators

Ultra-Small

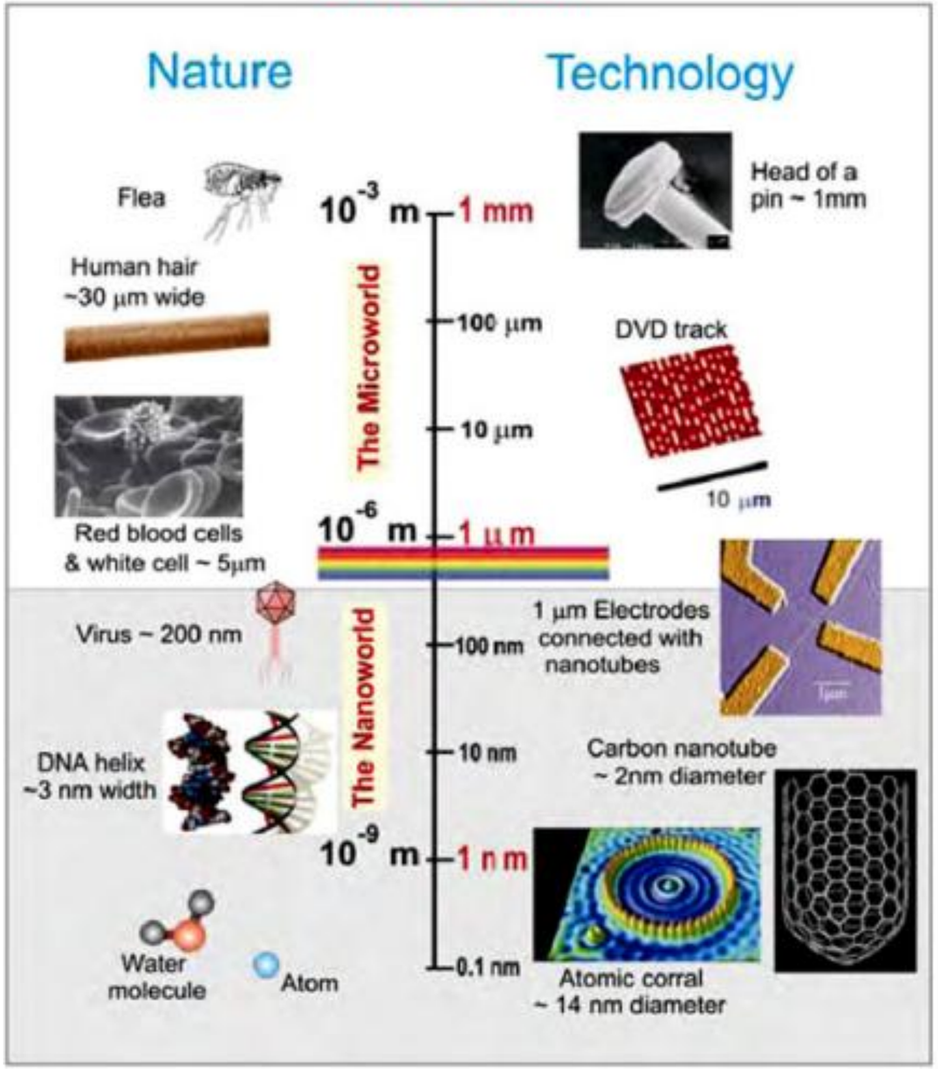

Ultra-Fast

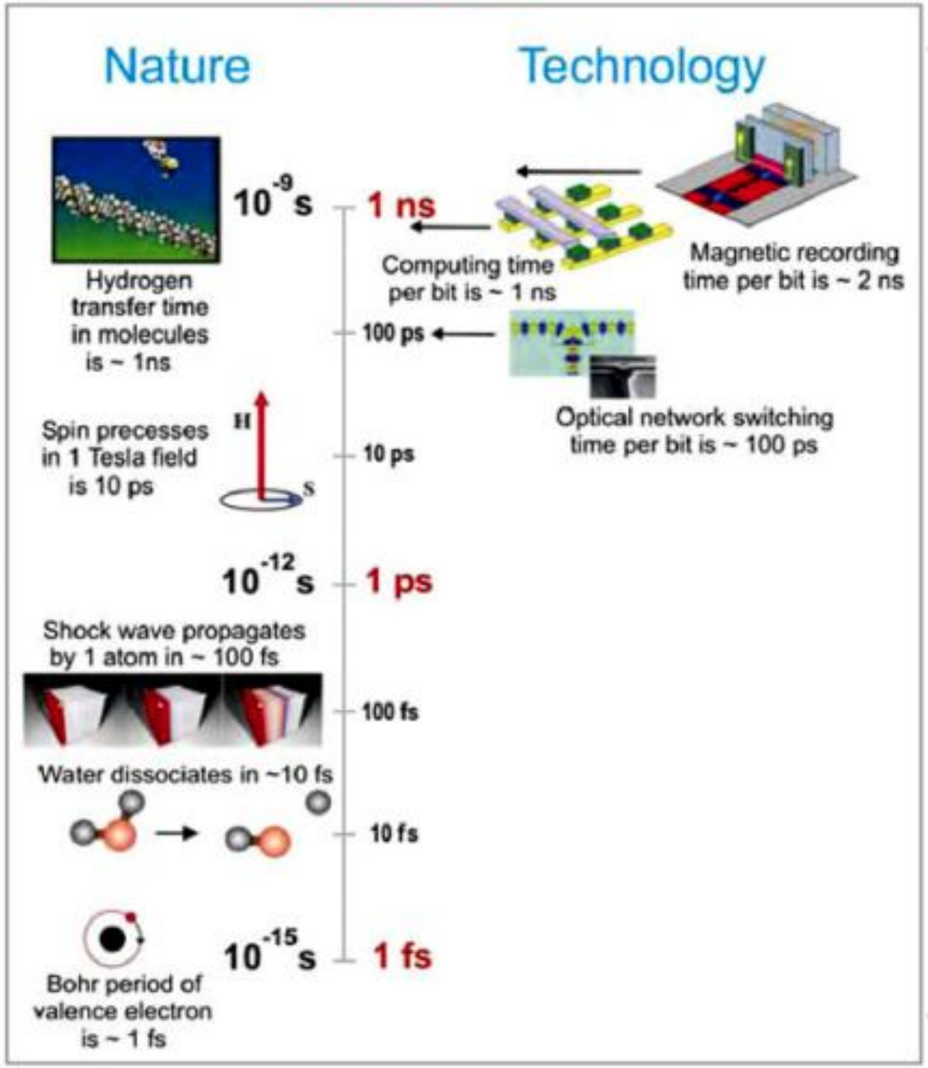

- ■ Simultaneous access to ultra-small spatial and ultra-fast temporal scales
- ■ Order of magnitude improvement in brightness, coherence, and tunability
- ■ From static structural analysis to dynamic process observation
- ■ Essential platform for materials, chemistry, biology, and quantum science

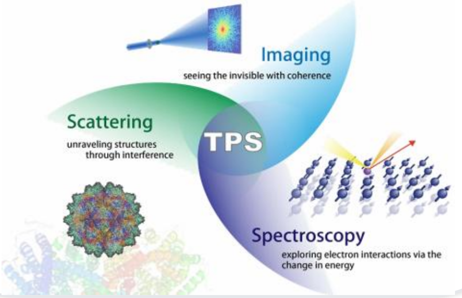

Core capabilities: High spatial resolution • High temporal resolution • High coherence & controllability

Future trend of Accelerator-based light source development

Intensity & Spectrum of Synchrotron Light

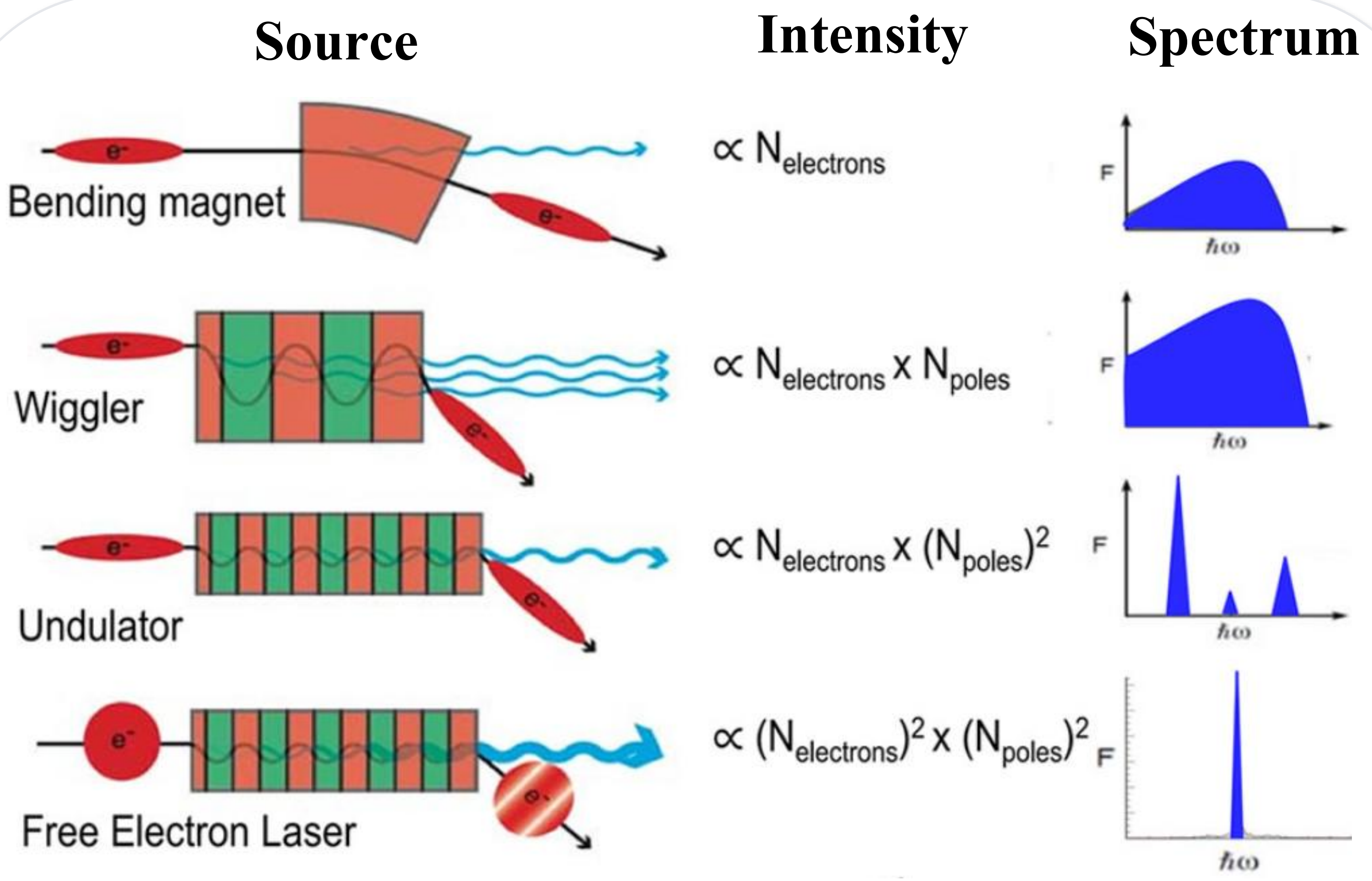

同步射光源自Dipole與Wiggler演進至Undulator與自由電子雷射，反映出相干性與相位關聯程度的逐步提升。

■Dipole與Wiggler屬非相干輻射，其強度隨電子數線性增加；

■Undulator器引入單電子相位干涉，在共振頻率形成窄頻譜線，強度隨 $NeNp^2$ 成長。

■自由電子雷射則透過電子–輻射場自洽耦合產生microbunching與相位鎖定，實現 Ne^2Np^2 的全相干增益，需極低能散與高增益條件，非僅低發射度即可達成

Synchrotron Facilities in the World

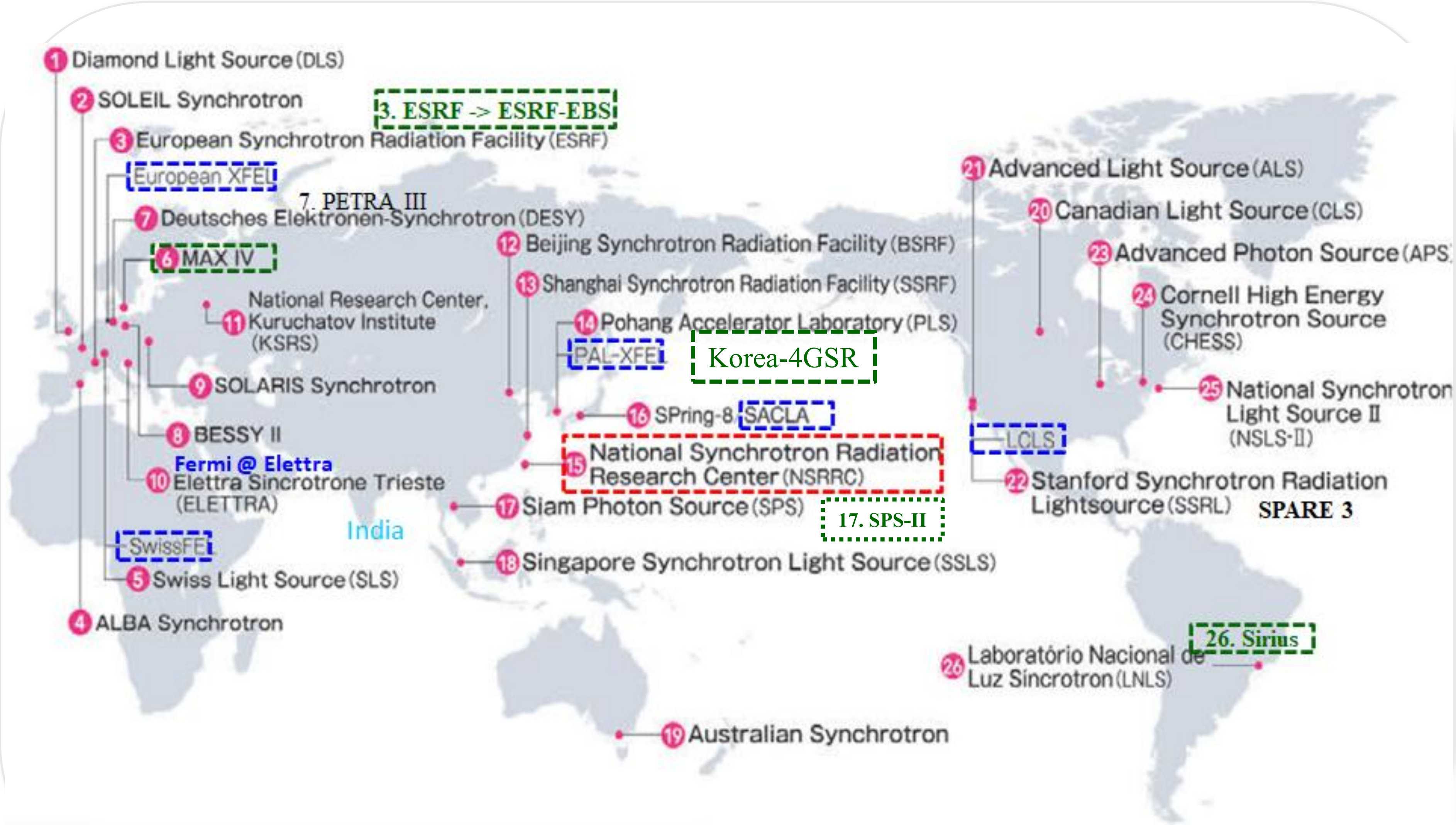

Ref: Encyclopedia of the Synchrotron Radiation Facilities

https://www.aps.anl.gov/sites/www.aps.anl.gov/files/APS-Uploads/2020SPring-ENCYCOLPEDIA_HIres.pdf

Synchrotron Light Source

自由電子雷射（FEL,藍色虛線)：

■ Linac-based、單脈衝極亮、完全相干

European XFEL
SwissFEL
PAL-XFEL
SACLA
LCLS -> LCLS-II

第四代繞射極限儲存環（DLSR,綠色虛線)：

MAX IV, Sirius
ESRF-EBS, APS-U, HEPS, SLS2
ALS-U

■ 低發射度 MBA lattice

■ 高 Brilliance + 可用相干性

光源指標：Flux、Brilliance、Coherent Fraction

- **Flux:** $\dfrac{number\ of\ photons}{\Delta t(0.1\%\ fractional\ bandwidth)}$

- **Brilliance:** defined as the ratio of the photon spectral flux to the volume of the convoluted phase of the electron beam and the photon beam in the two transverse dimensions, is given by

$$\text{Brilliance} = \frac{flux}{4\pi^2 \Sigma_x \Sigma_{x'} \Sigma_y \Sigma_{y'}}$$

$$\sigma_{x,e} = \sqrt{\epsilon_x \beta_x + (\eta_x \sigma_E)^2}$$

$$\sigma_{x',e} = \sqrt{\epsilon_x \gamma_x + (\eta'_x \sigma_E)^2}$$

$$\Sigma_x = \sqrt{\sigma_{x,e}^2 + \sigma_{ph}^2} \qquad \Sigma_{x'} = \sqrt{\sigma_{x',e}^2 + \sigma'^2_{ph}}$$

- **Coherent fraction (CF):** defined as the ratio of the square of photon wavelength to the volume of the convoluted phase of the electron beam and the photon beam in the two transverse dimensions, is also given by

$$\text{CF} = \frac{\lambda^2/(4\pi)^2}{\Sigma_x \Sigma_{x'} \Sigma_y \Sigma_{y'}}$$

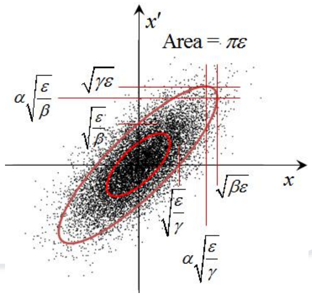

Flux：有多少光
Brilliance：光在相空間有多密
Coherent Fraction：光有多像雷射
第四代儲存環光源的關鍵不是更亮，而是可用相干性

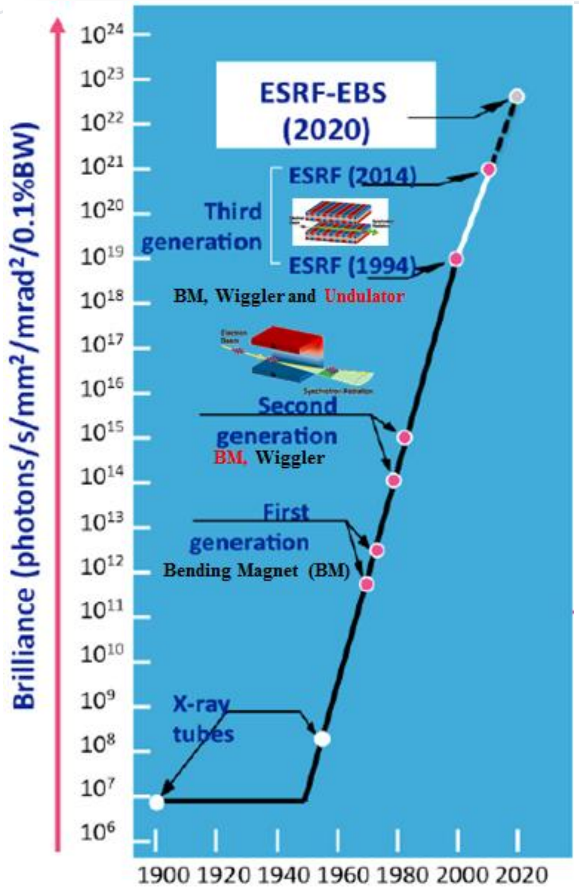

第一代光源源自高能物理儲存環中的寄生同步輻射

第二代光源為專用同步輻射光源

第三代光源進一步降低儲存環發射度，並配置長直線段以支援高性能 undulator

第四代光源，其核心特徵為繞射極限儲存環與自由電子雷射

Equilibrium Emittance of Storage Ring

The emittance is defined as **the area** occupied by the electron beam in the **phase space**

➢ Synchrotron Radiation integrals:

$$I_1 = \oint \frac{\eta_x}{\rho_x} ds \qquad I_3 = \oint \frac{1}{|\rho_x^3|} ds$$

$$I_2 = \oint \frac{1}{\rho_x^2} ds \qquad I_4 = \oint 2\frac{\eta_x k}{\rho_x} ds$$

$$I_5 = \oint \frac{\mathcal{H}_x}{|\rho_x^3|} ds$$

$$\mathcal{H} = \beta_x {\eta'_x}^2 + 2\alpha_x \eta_x \eta'_x + \gamma_x \eta_x^2$$

➢ Equilibrium emittance:

$$\epsilon_x = C_q \frac{\gamma^2 I_5}{I_2 - I_4} \propto \frac{E^2}{N_{Dipole}^3}$$

$$\propto E^2 \theta^3$$

➢ Energy spread:

$$\sigma_E^2 = C_q \frac{\gamma^2 I_3}{2I_2 + I_4}$$

ρ: the radius curvature of the dipole

η_x: Dispersion function

$$k = \frac{1}{B\rho} \frac{\partial B_y}{\partial x}$$

Beam Size

$$\sigma_{x,e} = \sqrt{\epsilon_x \beta_x + (\eta_x \sigma_E)^2}$$

$$\beta$$
$$\alpha \equiv -\beta'/2$$
$$\gamma \equiv \frac{1+\alpha^2}{\beta}$$

Lattice function (Twiss parameter)

第四代儲存環光源要在 emittance, dynamic aperture, Touschek lifetime, Nonlinearity之間做一個極端困難的多目標折衷

How to achieve lower emittance ring and its drawbacks:

- I_5 ↓ : Strong focusing / Chromaticity and lattice nonlinearity ↑
- I_2 ↑ : Damping wiggler, reverse bend / RF voltage ↑
- I_4 ↓ : Combined function (Dipole+Quad) / Energy spread ↑
- ρ ↑ : **More dipoles → MBA** / A lot of problems…

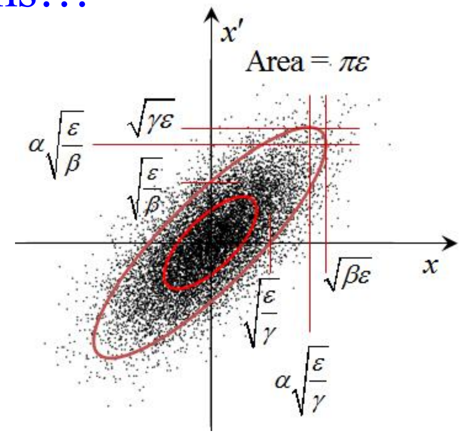

Equilibrium Emittance: balance between radiation damping and quantum excitation

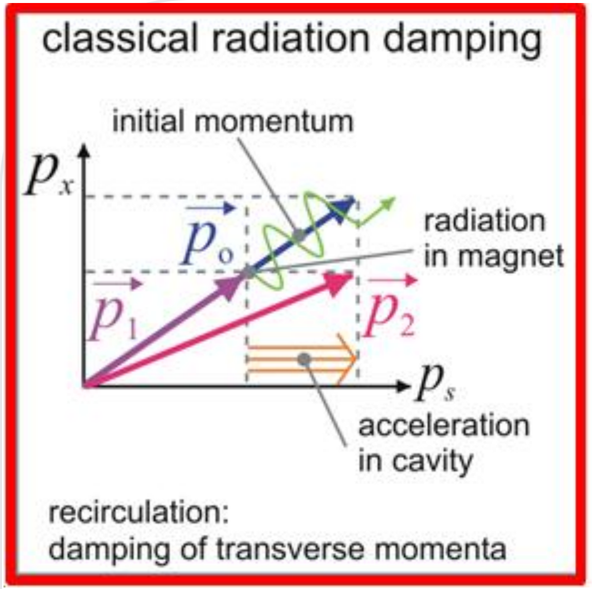

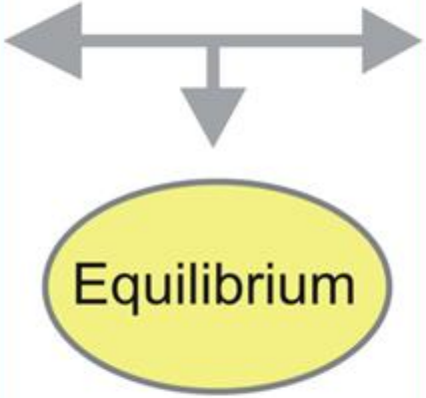

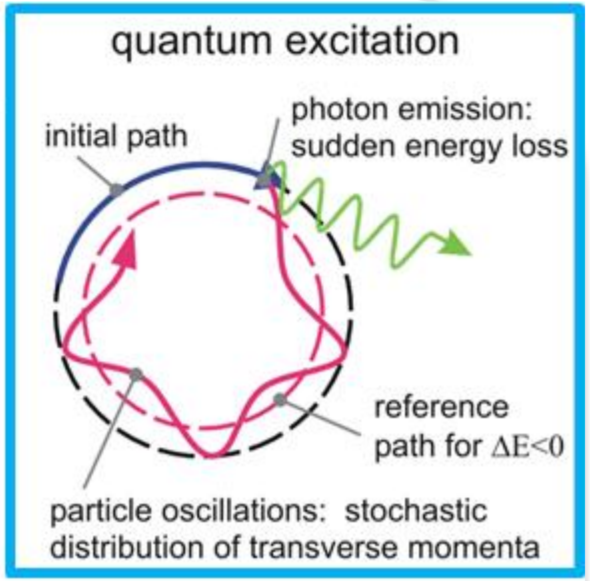

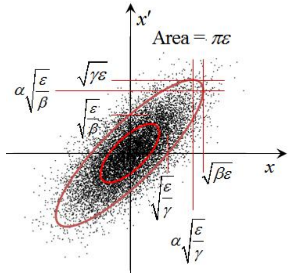

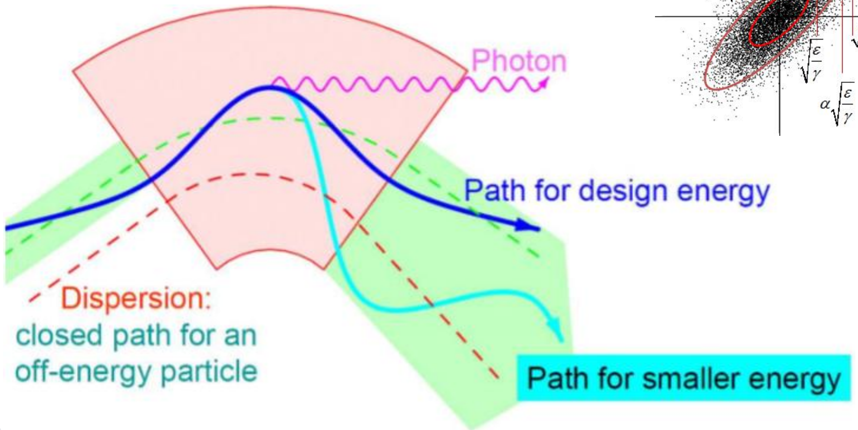

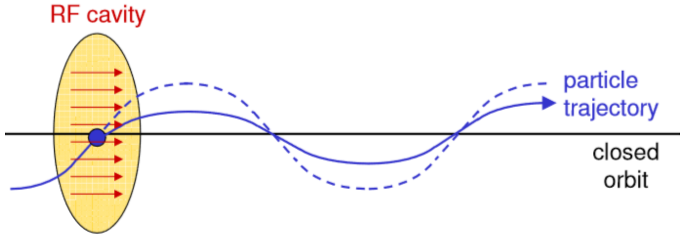

Slide courtesy of A. Streun, PSI

- Equilibrium emittance:

$$\epsilon_x = C_q \frac{\gamma^2 I_5}{I_2 - I_4} \propto \frac{E^2}{N^3_{Dipole}} \propto E^2 \theta^3$$

- Energy spread:

$$\sigma_E^2 = C_q \frac{\gamma^2 I_3}{2I_2 + I_4}$$

- Bunch length:

$$\sigma_s = \frac{\alpha_c c}{\omega_s} \sigma_\delta$$

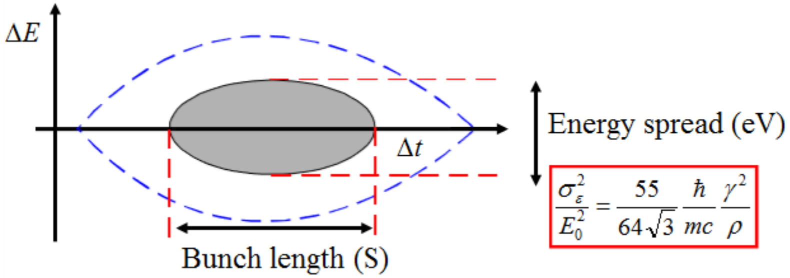

■**Linac-FEL**：因 single pass，無 recirculation,不存在rasiation damping與quantum excitation平衡,高增益 FEL 在有限距離內完成指數放大,以undulator長度換取相干度

Ultimate Storage Ring (USR)-> Diffraction Limited SR (DLSR)

Transverse emittance $\Sigma_{x,y}(\lambda)$ of X-ray beam from undulator (length L) is convolution of photon emittance ε_r from e- filament and e- emittance $\varepsilon_{x,y}$(e-) (Gaussian beams):

$$\Sigma_{x,y}(\lambda) = \varepsilon_r(\lambda) \oplus \varepsilon_{x,y}(e-) = \sqrt{\sigma_r^{\,2}(\lambda) + \sigma_{x,y}^{\,2}(e-)}\sqrt{\sigma'^{\,2}_r(\lambda) + \sigma'^{\,2}_{x,y}(e-)}$$

Here $\sigma_r(\lambda) \approx \frac{\sqrt{2\lambda L}}{2\pi}$ $\quad \sigma'_r(\lambda) = \sigma_\psi(\lambda) \approx \sqrt{\lambda/2L}$ Photon

---

$\sigma_{x,y}(e-) = \sqrt{\varepsilon_{x,y}\beta_{x,y}}$ $\quad \sigma'_{x,y}(e-) = \sqrt{\varepsilon_{x,y}/\beta_{x,y}}$ electron

Phase space matching conditions :

Transverse emittance $\Sigma_{x,y}$ minimized when $\varepsilon_{x,y}$ is minimized and photon and e- phase space orientations are matched:

$$\frac{\sigma_r(\lambda)}{\sigma'_r(\lambda)} = \frac{\sigma_{x,y}(e-)}{\sigma'_{x,y}(e-)} \Rightarrow \beta_{x,y} = \frac{L}{\pi}$$

Note: many authors cite $\beta_{x,y} = \frac{L}{2\pi}$

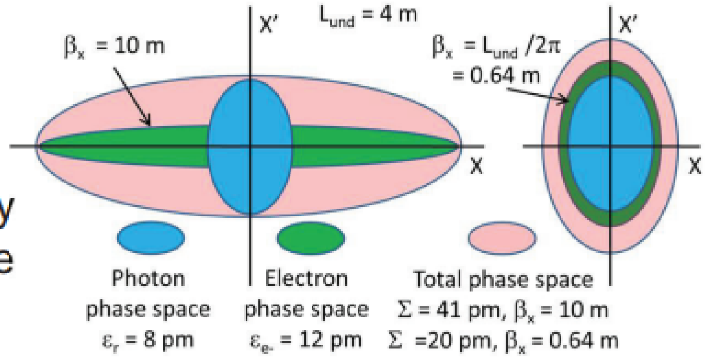

Ref: Perspectives and Challenges for Diffraction-Limited Storage Ring Light Sources, R. Hettel, M. Borland, MOYAB1, PAC2013, CA, USA https://epaper.kek.jp/PAC2013/talks/moyab1_talk.pdf

To approach the diffraction limit and increase the brightness of radiation, you need

- smaller electron beam emittance
- better phase space matching

between photon beam and electron beam

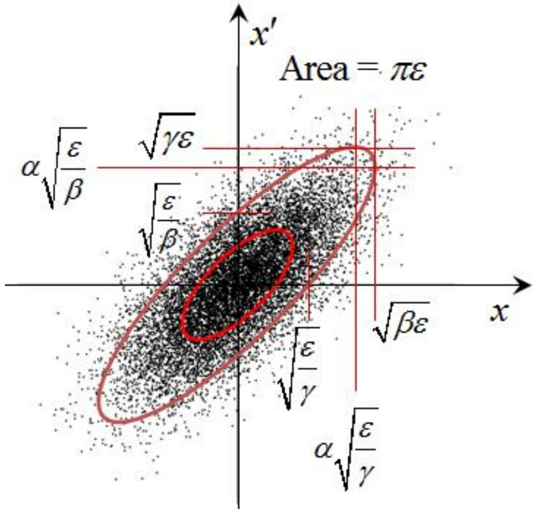

Trends of Storage Ring Light Sources

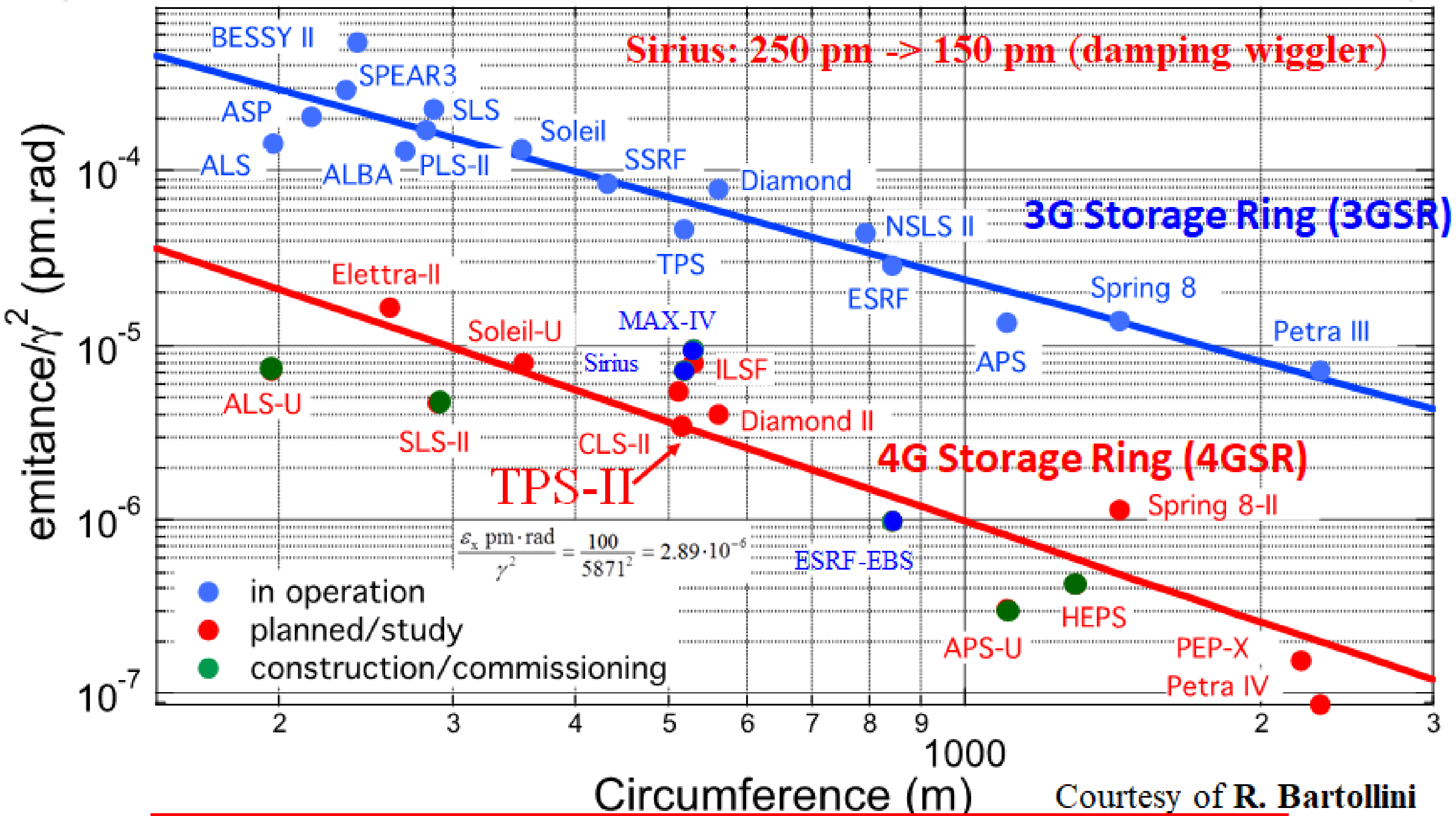

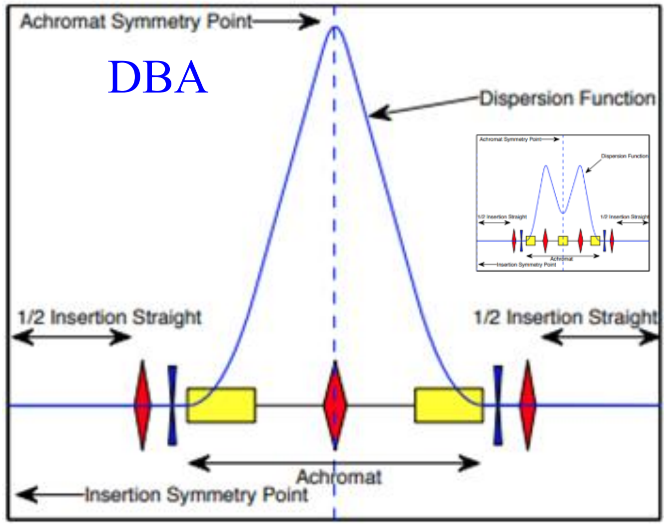

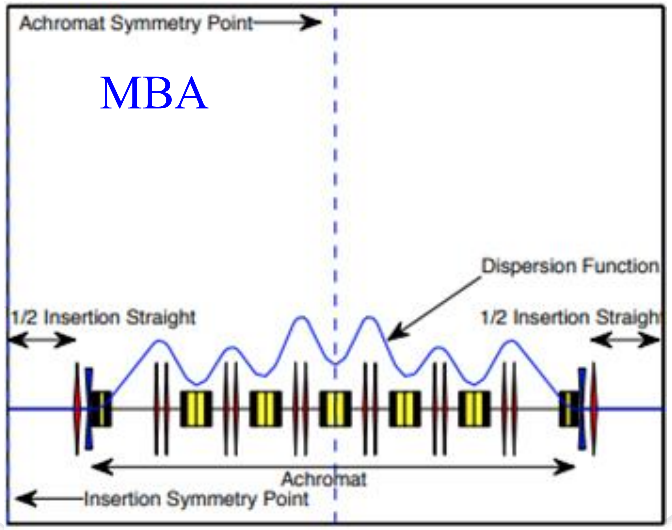

➢ Equilibrium emittance: $\epsilon_x = C_q \frac{\gamma^2 I_5}{I_2 - I_4} \propto \frac{E^2}{N^3_{Dipole}} \propto E^2 \theta^3$

https://proceedings.jacow.org/ipac2017/papers/tuxa1.pdf

Ref: Towards Diffraction Limited Storage Ring Based Light Sources, L. Liu† and H. Westfahl Jr. , 2017.

Trends of Storage Ring Light Sources

1. 7BA (MAX-IV): 3 GeV, 500 mA, 528 m, 7BA, 20 cells, emittance : 320 pm

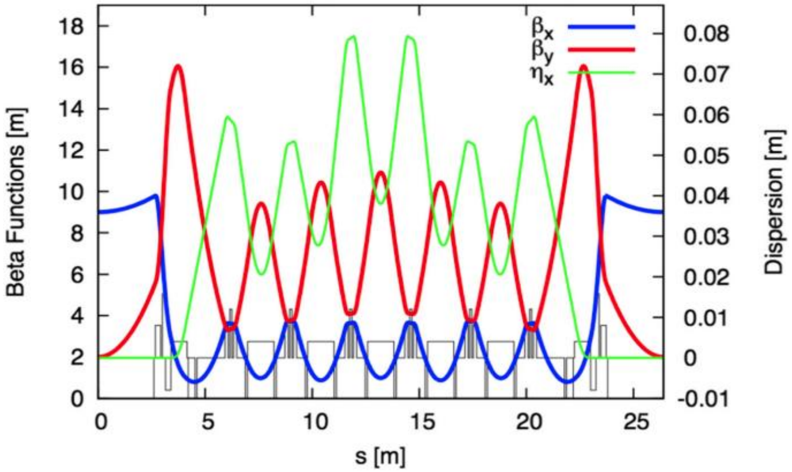

2. H7BA (ESRF-EBS, APS-U, HEPS, Korea-4GSR)

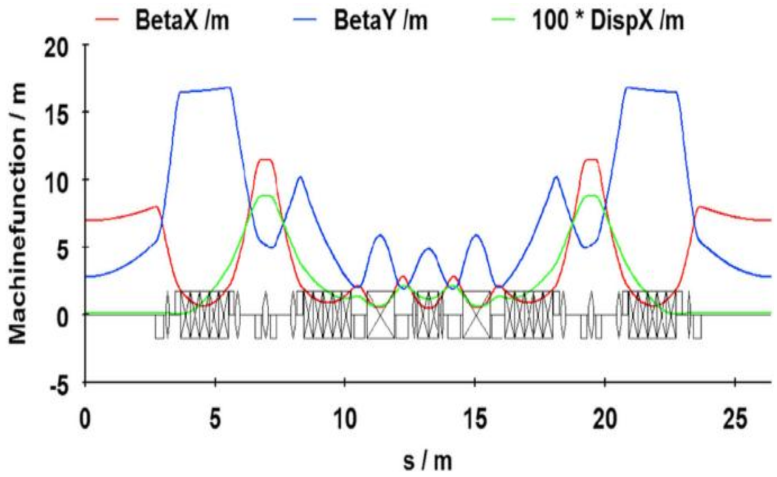

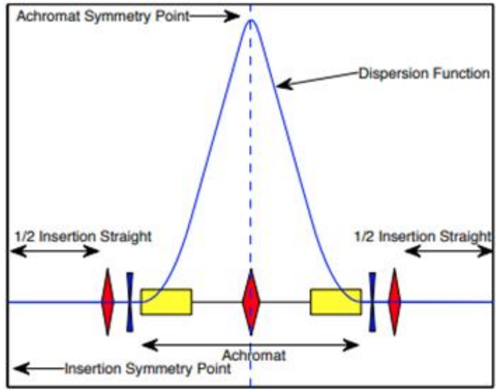

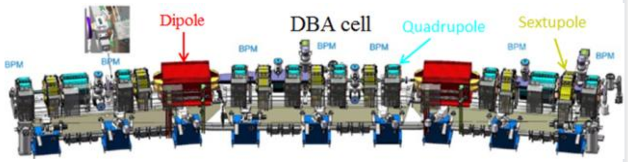

H6BA (PETRA IV,

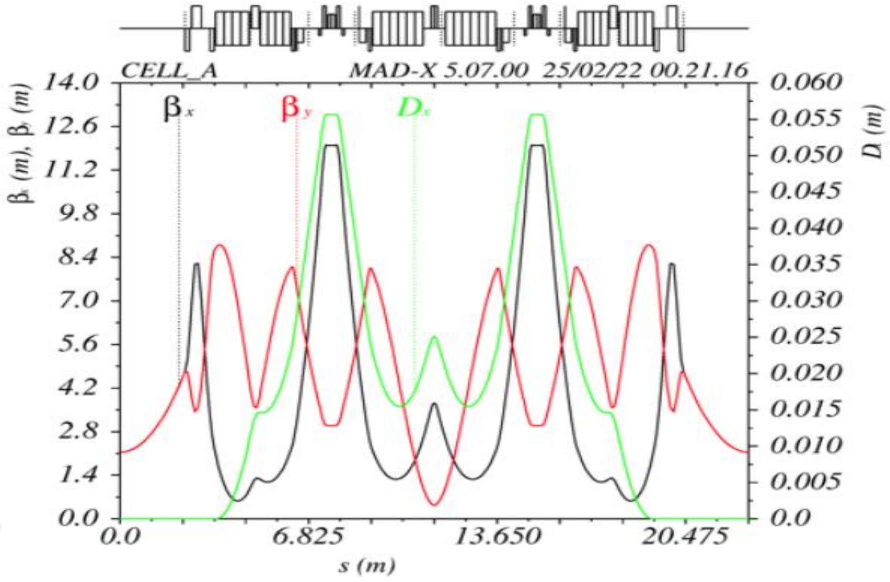

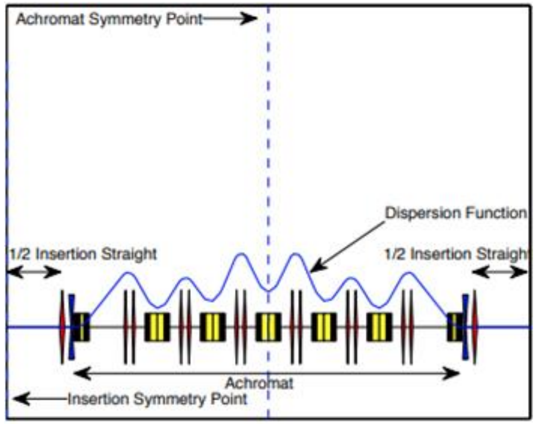

3. DTBA(Diamond II, SPS-II)

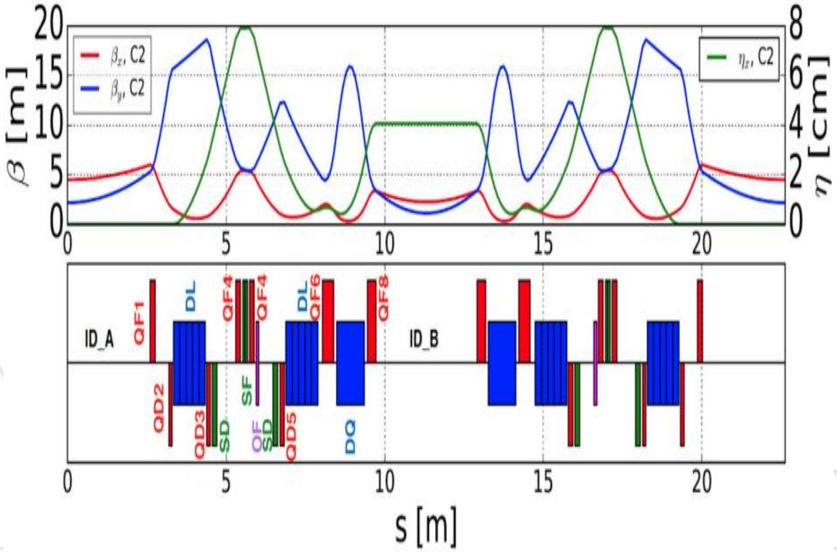

TPS Lattice

```
!TITLE, "TPS Booster Ring, NSRRC";

BEAM, PARTICLE=ELECTRON, ENERGY=3.0;

DL1:  DRIFT, L=6.000;
DL2:  DRIFT, L=0.730;
DL2A: DRIFT, L=0.355;
DL2B: DRIFT, L=0.125;
DL3:  DRIFT, L=0.700;
DL4:  DRIFT, L=0.750;
DL4A: DRIFT, L=0.125;
DL4B: DRIFT, L=0.375;
DC5:  DRIFT, L=0.550;
DC6:  DRIFT, L=0.950;
DC6A: DRIFT, L=0.275;
DC6B: DRIFT, L=0.425;
DC7:  DRIFT, L=0.255;
DS1:  DRIFT, L=3.500;
DS2:  DRIFT, L=0.680;
DS2A: DRIFT, L=0.305;
DS2B: DRIFT, L=0.125;
DS3:  DRIFT, L=0.800;
DS3A: DRIFT, L=0.425;
DS3B: DRIFT, L=0.125;
DS4:  DRIFT, L=0.320;

ANG:=7.5*PI/180;
BEND: SBEND, L=1.1, ANGLE:=ANG, K1=0.0, E1:=ANG/2, E2:=ANG/2;

QS5: QUADRUPOLE, L=0.3, K1= 1.610683E+00;
QS4: QUADRUPOLE, L=0.3, K1=-1.023454E+00;
QS3: QUADRUPOLE, L=0.3, K1=-1.312287E+00;
QS2: QUADRUPOLE, L=0.6, K1= 1.524420E+00;
QS1: QUADRUPOLE, L=0.3, K1=-1.624058E+00;
QL3: QUADRUPOLE, L=0.3, K1=-1.195106E+00;
QL2: QUADRUPOLE, L=0.6, K1= 1.281600E+00;
QL1: QUADRUPOLE, L=0.3, K1=-1.039134E+00;

SA: SEXTUPOLE, L=0.25, K2 = 11.891315760;
S1: SEXTUPOLE, L=0.25, K2 = 11.891315760;
S2: SEXTUPOLE, L=0.25, K2 =-27.952703592;
S3: SEXTUPOLE, L=0.25, K2 = 39.032799456;
S4: SEXTUPOLE, L=0.25, K2 =-42.294301920;
S5: SEXTUPOLE, L=0.25, K2 = 32.863032408;
S6: SEXTUPOLE, L=0.25, K2 =-40.675121112;
SD: SEXTUPOLE, L=0.25, K2 =-13.945200000*2;
SF: SEXTUPOLE, L=0.25, K2 = 19.152240000*2;

RF: RFCAVITY, L=0.1e-6, VOLT=3.5, LAG=0.5, HARMON=864; !, SHUNT=0.5, TFILL=25.0

LLONG: LINE=(DL1,QL1,DL2A,S1,DL2B,QL2,DL3,QL3,DL4A,S2,DL4B);
RLONG: LINE=(DS1,QS1,DS2A,S3,DS2B,QS2,DS3A,S4,DS3B,QS3,DS4);
HLACH: LINE=(DC5,QS4,DC6A,SD,DC6B,QS5,DC7,SF);
SHORT: LINE=(DS1,QS1,DS2A,S5,DS2B,QS2,DS3A,S6,DS3B,QS3,DS4);
HSACH: LINE=(DC5,QS4,DC6A,SD,DC6B,QS5,DC7,SF);
HSACH1:LINE=(DC5,QS4,DC6A,SD,DC6B,QS5,DC7);

MMC:marker;
MM: marker;
M : marker;
MP: marker;
MS: marker;

LCELL: LINE=(LLONG, MMC, BEND, HLACH, MM, -HSACH1, BEND, MMC, -RLONG);
SCELL: LINE=(SHORT, MMC, BEND, HSACH, MM, -HSACH1, BEND, MMC, -SHORT);

SUPERA: LINE=(MS,LCELL,M,SCELL,M,-SCELL,M,-LCELL,MP);

RING:   LINE=(3*SUPERA,RF,3*SUPERA);

!DX10:STRING,"DX*10"

USE, PERIOD=SUPERA;
SELECT,flag=twiss,column=name,s,betx,bety,alfx,alfy,mux,muy,dx;
TWISS,file= "TPS_SR_twiss.txt",SEQUENCE=SUPERA;
PLOT,HAXIS=S, VAXIS1=BETX,BETY, VAXIS2=DX, HMIN=0, HMAX=86.4, colour=100, style=1, interpolate;


USE, PERIOD=SCELL;
SELECT,flag=twiss,column=name,s,betx,bety,alfx,alfy,mux,muy,dx;
TWISS,file= "TPS_SR_SS_twiss.txt",SEQUENCE=SCELL;
PLOT,HAXIS=S, VAXIS1=BETX,BETY, VAXIS2=DX, HMIN=0, HMAX=20.16, colour=100, style=1, interpolate;


USE, period=SUPERA;
SAVEBETA,LABEL=ML,PLACE=MS, SEQUENCE=SUPERA;
TWISS;
SHOW,ML;

INITIAL: BETA0, BETX=ML->BETX, ALFX=ML->ALFX, MUX=0, BETY=ML->BETY, ALFY=ML->ALFY, MUY=0, DX=ML->DX, DPX=ML->DPX, DY=ML->DY, DPY=ML->DPY;
SHOW,INITIAL;

USE, PERIOD=LCELL;
SELECT,flag=twiss,column=name,s,betx,bety,alfx,alfy,mux,muy,dx;
TWISS,BETA0=INITIAL,file= "TPS_SR_LS_twiss.txt",SEQUENCE=LCELL;
PLOT,HAXIS=S, VAXIS1=BETX,BETY, VAXIS2=DX, HMIN=0, HMAX=43.2-20.16, colour=100, style=1, interpolate;
```

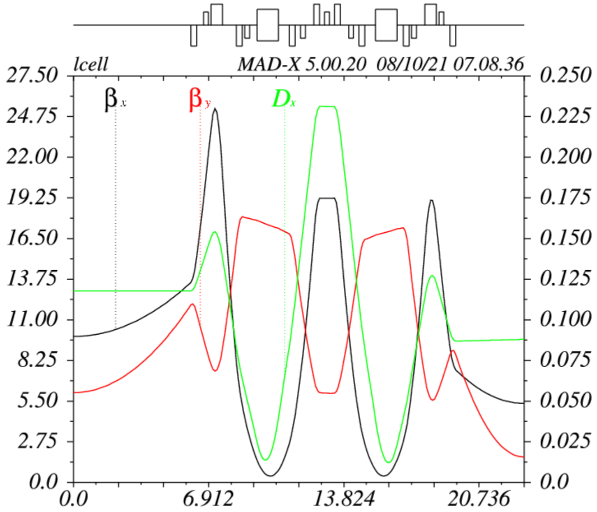

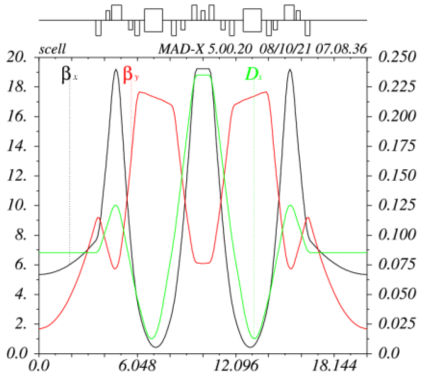

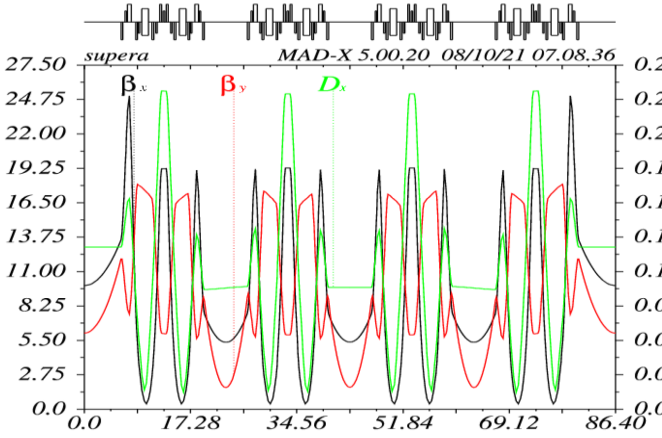

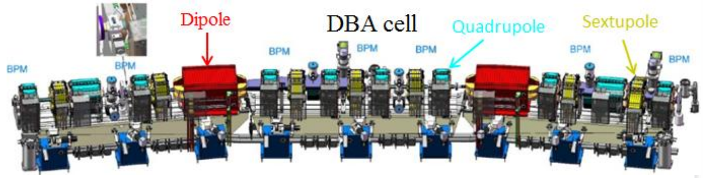

https://madx.web.cern.ch/

TPS upgrade Study

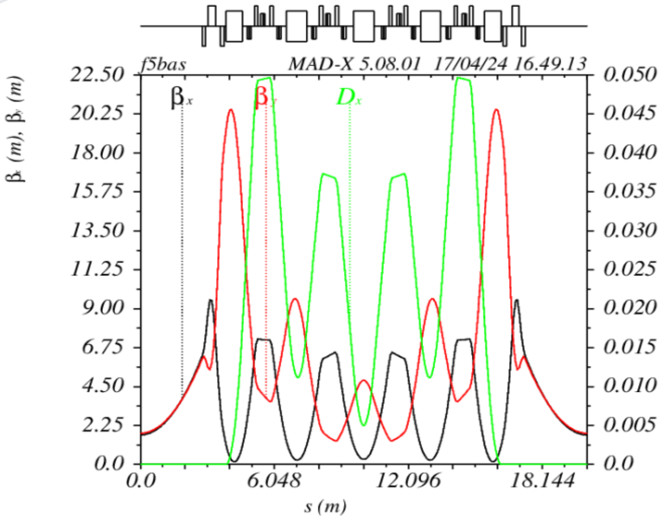

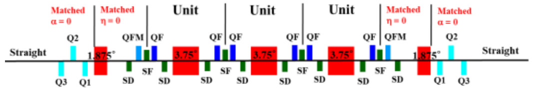

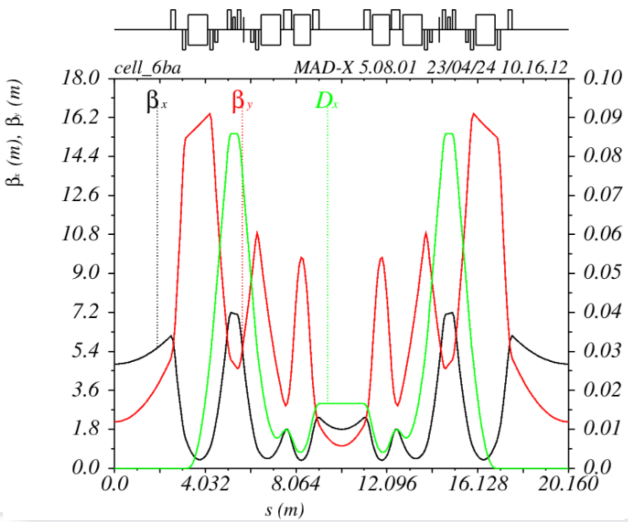

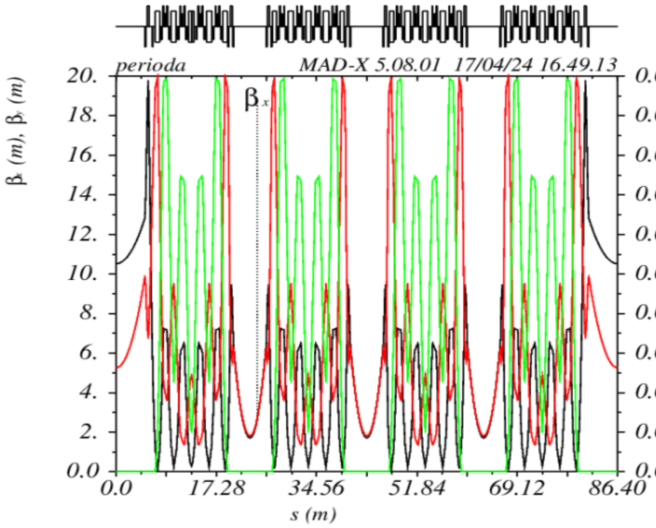

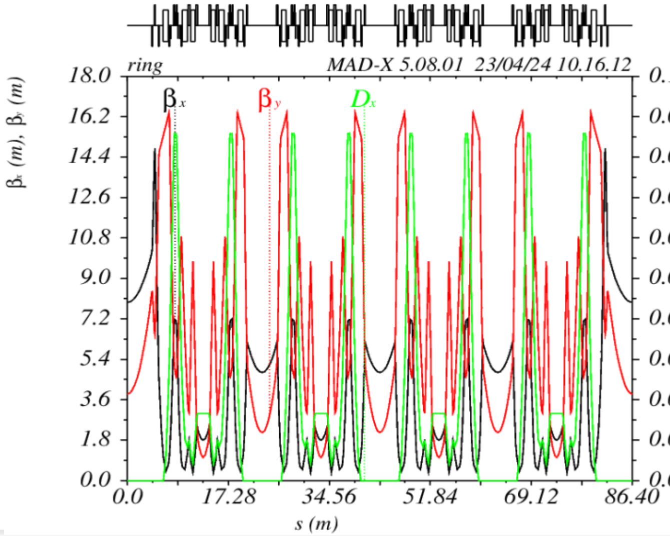

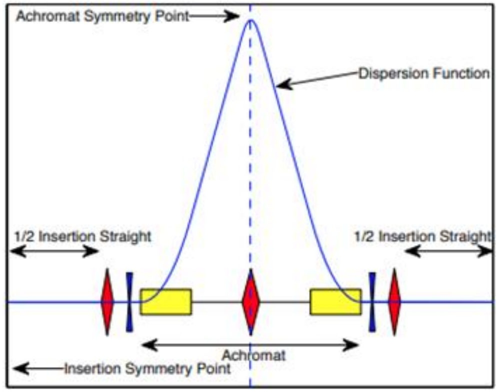

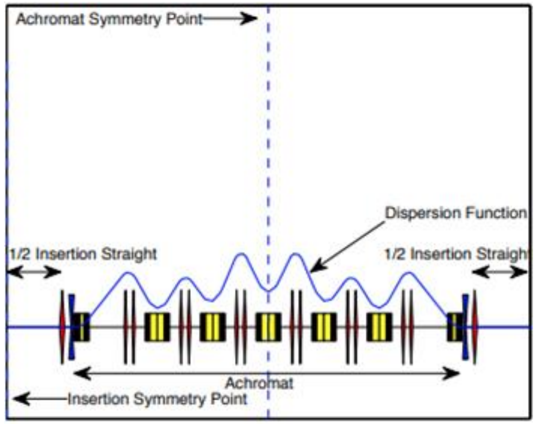

https://meow.elettra.eu/81/pdf/MOPB055.pdf

Lattice Design Trends for 4GSR (4G Storage Ring)

Table 1 Worldwide ongoing 4GSR projects [25]

Ref: New era of synchrotron radiation: fourth-generation storage ring, Seunghwan Shin. 30 August 2021

	Energy (GeV)	Emittance (pm)	Ener. spr. (1e− 4)	Beta x/y (m) @ source point	DA (mm)/beta x (m) @ inj. point	LMA (%)/TL (h)	Mcf (1e− 5)	Reverse bends	ID source point move
ALS-U	2.0	108	9.8	2.0/2.8 9BA	1.0/2.0	2.5/1.0	27	Yes	No
ELETTRA 2	2.4	212	9.3	5.7/1.6	6.0/5.7	4.0/6.2	12	Yes	No
SLS-II	2.7	157	12.0	2.5/1.3	7.0/22.0	4.0/6.3	10.4	Yes	< 70 mm
SOLEIL-U	2.75	81	9.0	1.3/1.3	5.0/11.0	3.5/3.3	9.1	Yes	< 100 mm
SIRIUS	3	250	8.5	1.5/1.5	10.0/17.0	3.7/3.9	16.0	No	n/a
Diamond-II	3.5	136	9.0	6.0/2.5	5.0/6.0	1.6/4.0	11	Yes	No
APS-U	6	42	13.5	4.9/1.9	2.2/5.2	2.1/4.0	4.0	Yes	No
ESRF-EBS	6	135	9.3	6.9/2.6	8.0/18.6	3.4/20	8.5	No	No
HEPS	6	< 60 (35)	10	2.6/2.3	1.0/2.6	1.5/1.0	1.8	Yes	n/a
PETRA-IV	6	20	11.2	4.0/2.0	3.6/21.7	2.0/1.2	1.6	tbd	Yes

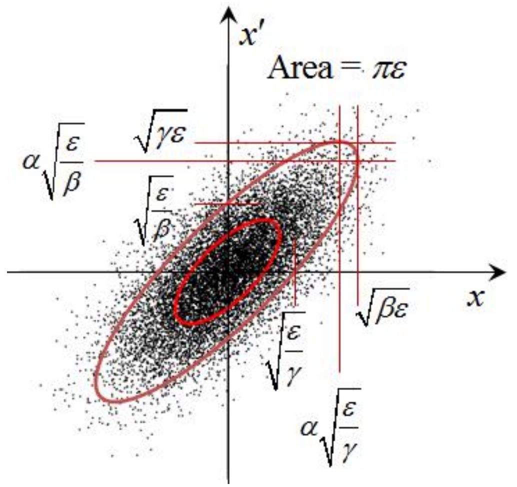

Coherence fraction:
phase space matching

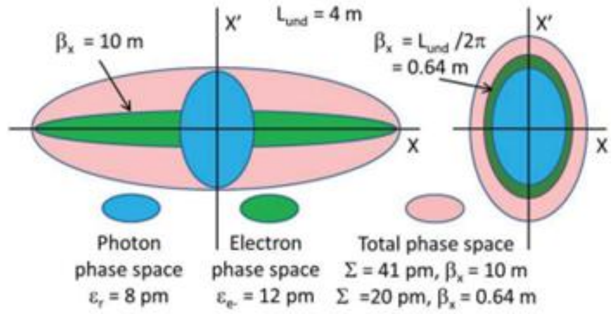

- **Energy Range:** Storage ring energies range from 2 to 6 GeV.
- **Emittance**: Emittances are below 300 pm, with PETRA-IV achieving a minimum emittance of 20 pm, aided by its large circumference.
- **Lattice Design Trends**:
  - Implementation of **reverse bends** is a common trend to increase radiation damping and tunability for β-function and dispersion function .
  - Not all machines optimize the beta function for **phase space matching** between the electron and photon beams.
  - Some machines feature large horizontal beta-functions at the injection point for easier beam injection.

Magnet Design Trends for 4GSR (4G storage Ring)

Table 2 Magnet field summary for 4GSR [25]

	Energy (GeV)	MAX b′ (T/m)	MAX b″ (T/m^2)	MAX b‴ (T/m^3)	Min. bore radius (mm)
ALS-U	2.0	105	10,500	n/a	12.0
ELETTRA 2	2.4	50	4000	45,000	13.0
SLS-II	2.7	97	8000	270,000	10.5
SOLEIL-U	2.75	< 110	16,000	1,500,000	8.0
SIRIUS	3	45	2400	n/a	14.0
Diamond-II	3.5	85	7700	660,000	12.0
ESRF-EBS	6	90	3200	37,000	12.8
HEPS	6	80	7500	670,000	12.5
PETRA-IV	6	92	6400	330,000	12.5
APS-U	6	86	6300	n/a	13.0

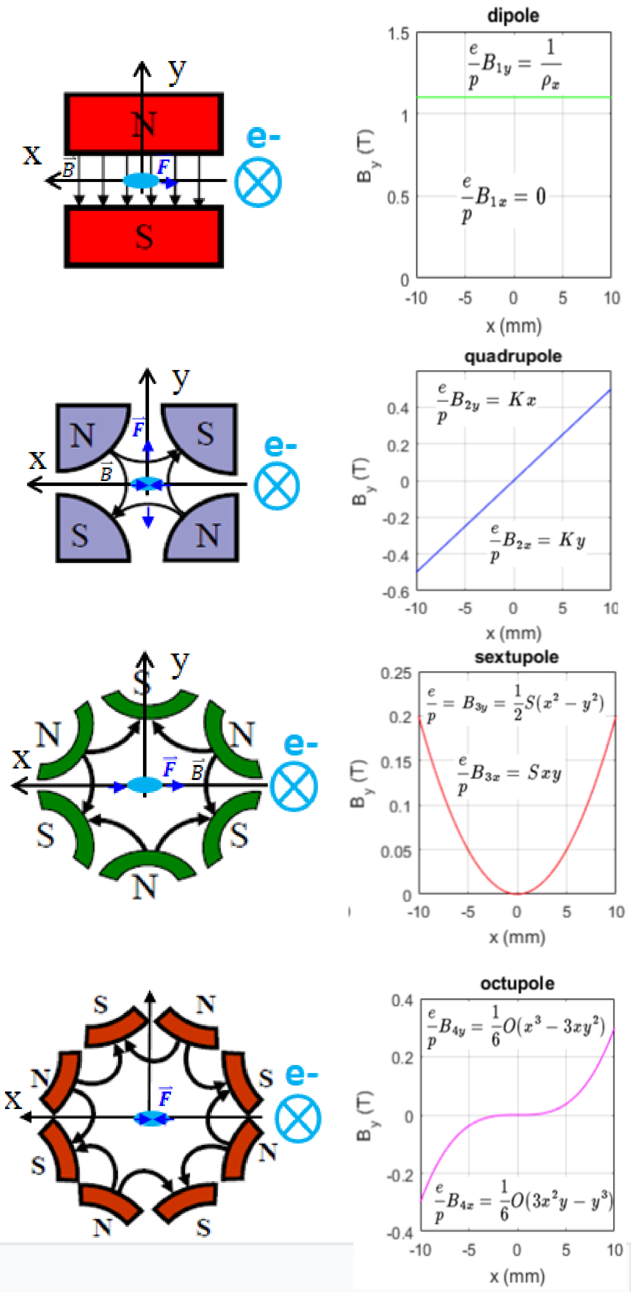

- **High Gradient Magnets:** Strong focusing quadrupoles with gradients up to 100 T/m are essential. These magnets often have very small bore apertures to achieve high design fields. The design and engineering integration are complex, accommodating photon extraction pipes, adjacent magnets, and other lattice elements (flanges, gate valves, vacuum pumps, absorbers, and BPMs).
- **Octupoles:** Used to control higher-order chromatic effects.
- **Longitudinal Gradient Magnets:** Necessary to further reduce emittance.
- **Permanent Magnets:** Considered for sustainability and energy efficiency.
- Small Bore radius: Require higher precision in manufacturing and alignment.

Ref: New era of synchrotron radiation: fourth-generation storage ring, Seunghwan Shin. 30 August 2021

Vacuum Chamber and Collective Effects: Wakefield & Impedance

Wakefield (time domain) & Impedance (frequency domain) :

$$Z_{\parallel}(\omega) = \frac{Z_0 c}{4\pi}\int_{-\infty}^{+\infty} W_{\parallel}(z) e^{-i\frac{\omega z}{c}} \frac{dz}{c}$$

$$Z_{\perp}(\omega) = i\frac{Z_0 c}{4\pi}\int_{-\infty}^{\infty} W_{\perp}(z) e^{-i\frac{\omega z}{c}} \frac{dz}{c}$$

$$Z_{\parallel}(\omega) = \frac{\omega}{c} Z_{\perp}(\omega)$$

Narrow band Impedance: (Cavity)

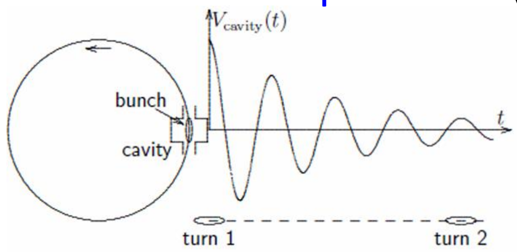

$$Z_{\parallel}(\omega) = \frac{R_s}{1 + iQ\left(\frac{\omega_r}{\omega} - \frac{\omega}{\omega_r}\right)}$$

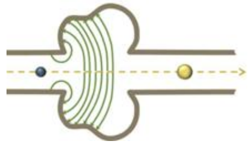

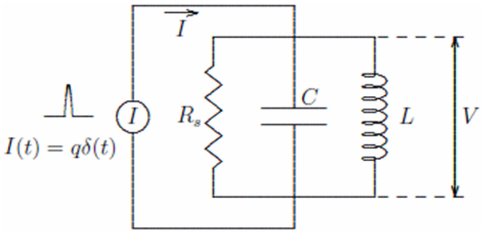

Resistive Wall Impedance:

Finite conductivity of chamber wall; long-range wake

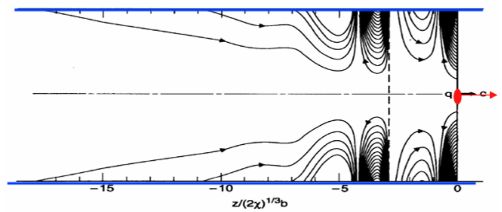

$$Z_{\perp}^{RW}(\omega) \approx (1+i)\frac{Z_0}{\pi b^3}\sqrt{\frac{c}{2\sigma\mu_0\,\omega}}$$

$$Z_{\parallel}^{RW}(\omega) \approx (1+i)\frac{Z_0}{2\pi b}\sqrt{\frac{\omega}{2\sigma\mu_0}}$$

$$Z_{\perp}(\omega) = \frac{1}{\pi b^3}\sqrt{\frac{2\pi}{\sigma|\omega|}}[sgn(\omega) - i]$$

Instability:

$$\ddot{y}_n(t) + \omega_\beta^2 y_n(t) = -\frac{r_0 c}{\gamma T_0}\sum_{k=-\infty}^{\infty}\sum_{m=0}^{M-1} N a_m W_{\perp}\left(-kC - \frac{m-n}{M}C\right) \times y_m\left(t - kT_0 - \frac{m-n}{M}T_0\right)$$

$$(\Omega - \omega_\beta)\tilde{y}_n = -i\frac{N r_0 c}{2\gamma T_0^2 \omega_\beta}\sum_{m=0}^{M-1} a_m \tilde{y}_m \sum_{p=-\infty}^{\infty} Z_{\perp}(p\omega_0 + \omega_\beta)\exp\left(-i2\pi p\frac{m-n}{M}\right)$$

$$y_n(t) = \tilde{y}_n e^{-i\Omega t}, \quad \Omega \approx \omega_\beta$$

$$\Delta\omega_n^{\mu} = \Omega_n^{\mu} - \omega_\beta = -i\frac{a_m M N r_0 c}{2\gamma T_0^2 \omega_\beta}\sum_{p=-\infty}^{\infty} Z_{\perp}[(pM + u)\omega_0 + \omega_\beta]$$

Beam Spectrum:

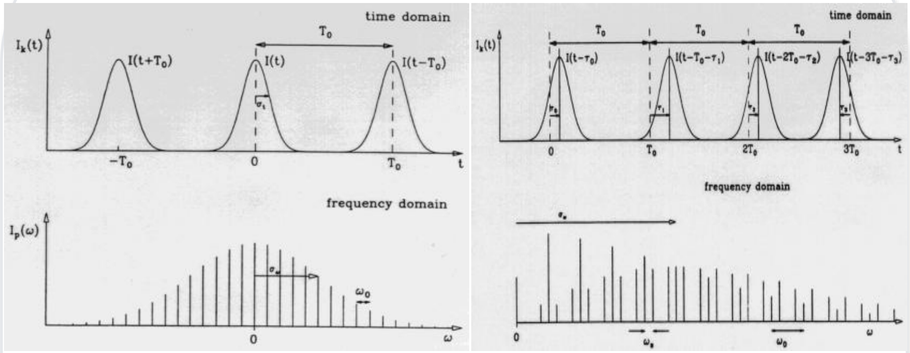

$$t \rightarrow t + \hat{\tau}\cos(\omega_s t) \;\Rightarrow\; I_k(t) = \sum_{p=-\infty}^{\infty} I_p e^{ip\omega_0[t+\hat{\tau}\cos(\omega_s t)]}$$

$$I_k(t) \simeq 2\sum_{\omega>0} I_p\left[\cos(p\omega_0 t) + \frac{p\omega_0\tau}{2}\sin((p+Q_s)\omega_0 t) + \frac{p\omega_0\tau}{2}\sin((p-Q_s)\omega_0 t)\right]$$

ω_p^+ $\quad$ ω_p^-

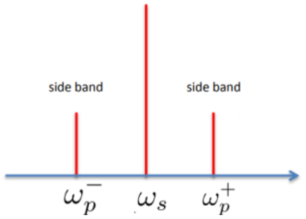

$$\left|\frac{Z_{\parallel}}{n}\right|_{eff} = \frac{\int\left|\frac{Z_{\parallel}}{n}\right| h_m dn}{\int h_m dn}$$

$$h_m = \frac{1}{\Gamma\left(m + \frac{1}{2}\right)}(n\omega_0\sigma_{z0}/c)^{2m} e^{-(n\omega_0\sigma_{z0}/c)^2}$$

The transverse impedance can be related to the longitudinal impedance for a circular pipe of radius b by:

$$Z_{\perp}(\omega) = \frac{2c}{b}\frac{Z_{\parallel}(\omega)}{\omega}$$

Vacuum Chamber and Collective Effects: Wakefield & Impedance

Narrow-Band Impedance:

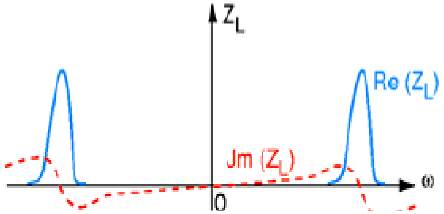

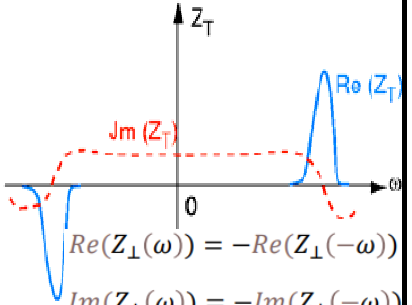

$Re(Z_\parallel(\omega)) = Re(Z_\parallel(-\omega))$

$Im(Z_\parallel(\omega)) = -Im(Z_\parallel(-\omega))$

$Re(Z_\perp(\omega)) = -Re(Z_\perp(-\omega))$

$Im(Z_\perp(\omega)) = -Im(Z_\perp(-\omega))$

Discrete cavity HOMs, trapped modes, high-Q structures, RF cavity

$$Z(\omega) \approx R_s \frac{1 - i2Q\frac{\Delta\omega}{\omega_r}}{1 + \left(2Q\frac{\Delta\omega}{\omega_r}\right)^2}$$

with $\Delta\omega = n\omega_0 - \omega_r$

$$\left|\frac{Z_\parallel}{n}\right|_{eff} = \frac{\int \left|\frac{Z_\parallel}{n}\right| h_m dn}{\int h_m dn}$$

$$y_n(t) = \tilde{y}_n e^{-i\Omega t}, \quad \Omega \approx \omega_\beta$$

$$h_m = \frac{1}{\Gamma\left(m + \frac{1}{2}\right)} (n\omega_0 \sigma_{z0}/c)^{2m} e^{-(n\omega_0\sigma_{z0}/c)^2}$$

Broad-Band Impedance:

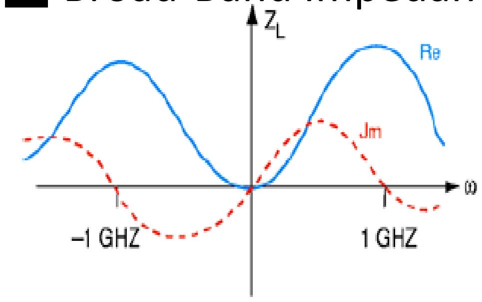

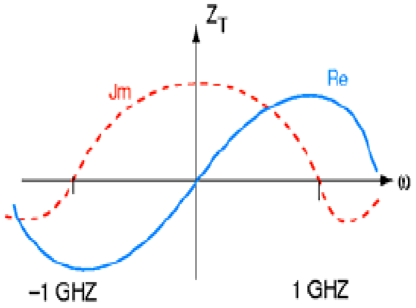

Short discontinuities (**bellows**, **tapers**, BPMs, etc.), low-Q effective model

$$Z(\omega) = R_s \frac{1 - iQ\frac{\omega^2 - \omega_r^2}{\omega\omega_r}}{1 + \left(Q\frac{\omega^2 - \omega_r^2}{\omega\omega_r}\right)^2} \qquad Q \approx 1 \quad \omega_r \approx 1\ \text{GHz}$$

Microwave instability (longitudinal) threshold:

$$I_{\text{threshold}} = \frac{\sqrt{2\pi}\,\alpha_c \sigma_z (E/e)}{R\left|Z_\parallel/n\right|_{bb}} \left(\frac{\sigma_e}{E}\right)^2$$

Fast head tail instability (transverse) threshold:

$$I_{\text{threshold}} = \frac{\sqrt{2\pi}\alpha_c (E/e)}{\left\langle \beta |Z_\perp|_{bb} \right\rangle} \left(\frac{\sigma_e}{E}\right)$$

Resistive Wall Impedance: beam pipe

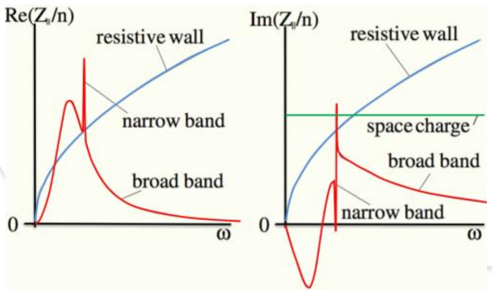

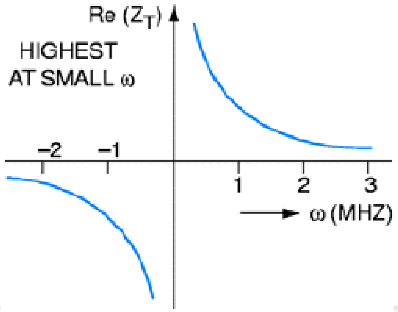

Finite conductivity of chamber wall; long-range wake

$$Z_\perp^{RW}(\omega) \approx (1+i)\frac{Z_0}{\pi b^3}\sqrt{\frac{c}{2\sigma\mu_0\,\omega}}$$

$$Z_\parallel^{RW}(\omega) \approx (1+i)\frac{Z_0}{2\pi b}\sqrt{\frac{\omega}{2\sigma\mu_0}}$$

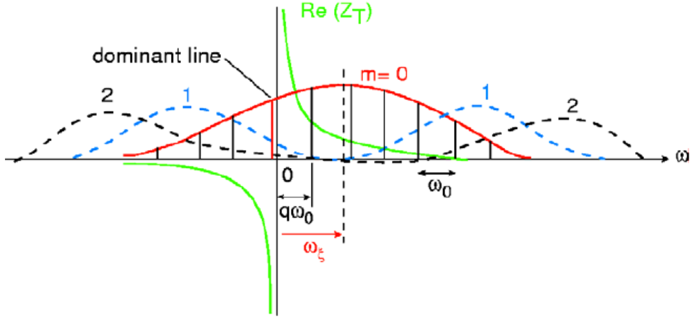

The transverse impedance can be related to the longitudinal impedance for a circular pipe of radius b by: $Z_\perp(\omega) = \frac{2c}{b}\frac{Z_\parallel(\omega)}{\omega}$

RF cavity trends for 4GSR: Main + Harmonic Cavity

■**Purpose:** Harmonic cavities used to flatten the RF potential to lengthen the bunches
- Longer Touschek lifetime
- Less intra-beam scattering
- Reduced heating of vacuum components

■Type of Harmonic cavity

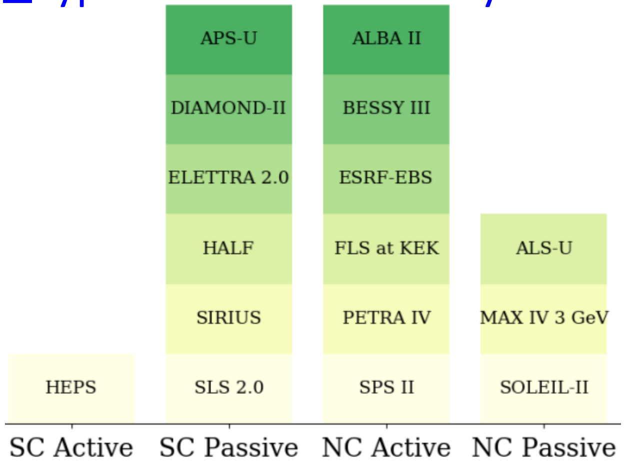

■Fill pattern

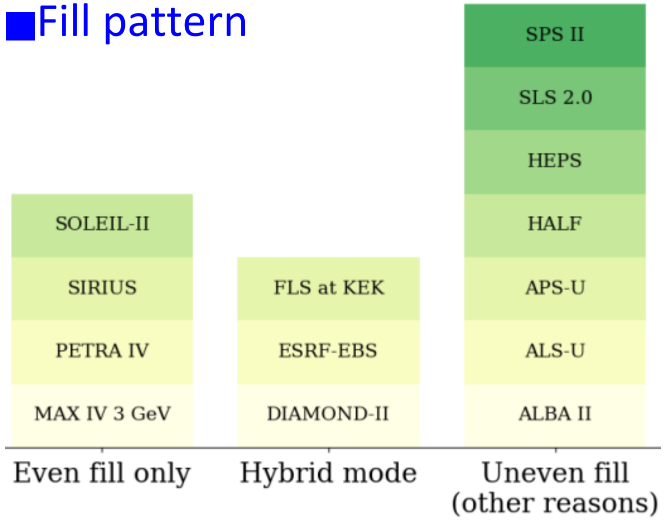

https://proceedings.jacow.org/fls2023/papers/mo2l3.pdf

Ref: Review of Harmonic Cavities in Fourth-Generation Storage Rings, F. J. Cullinan∗, Å. Andersson, P. F. Tavares, MAX IV Laboratory, Lund, Sweden, FLS23

https://journals.aps.org/prab/pdf/10.1103/PhysRevSTAB.4.030701

J. M. Byrd & M. Georgsson, PRSTAB 4 030701 (2001)

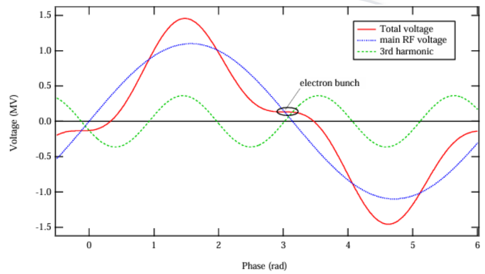

■TPS HC 發展

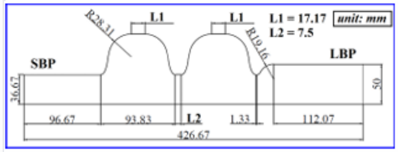

Courtesy of Zong-Kai Liu

~2016 模擬工具開發與驗證

2016-18: 雙腔cavity設計與優化

2020-21: Nb cavity由日本MHI MS 製造

2025: 組裝完成

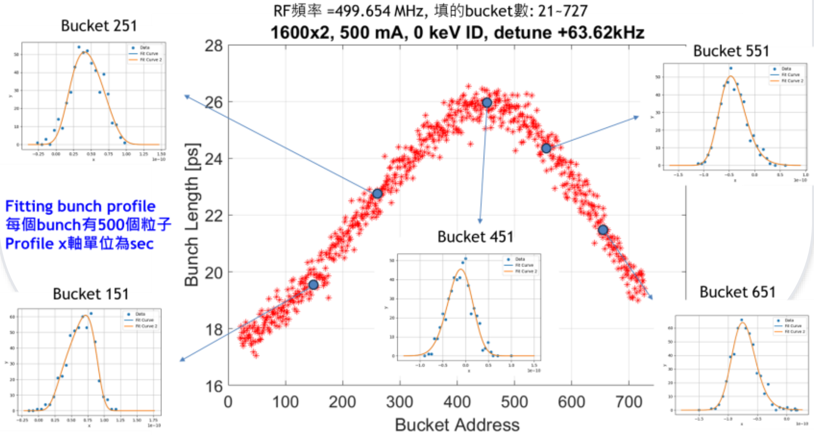

Lattice Design Summary

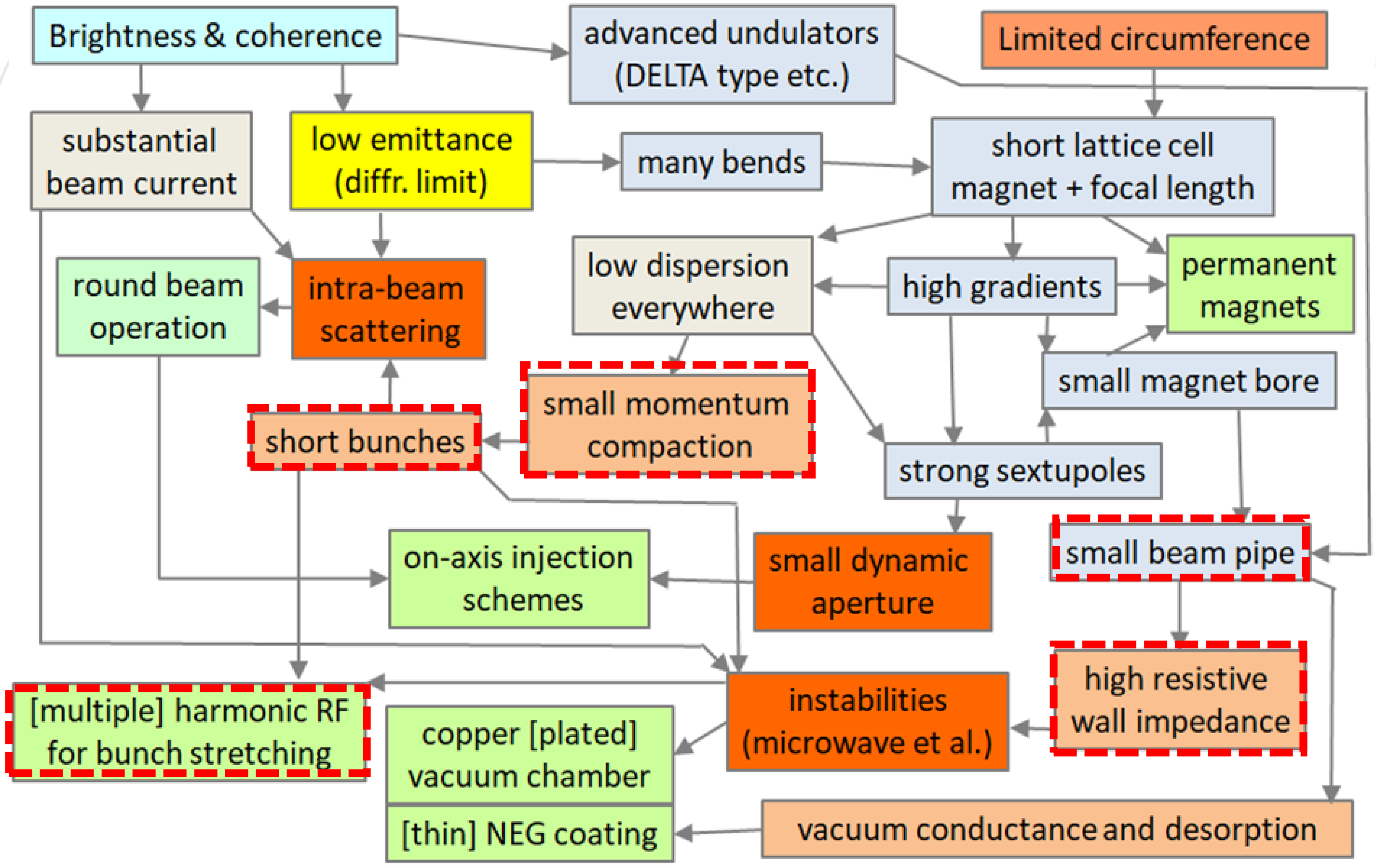

第四代儲存環光源要在 emittance, dynamic aperture, Touschek lifetime, nonlinearity之間做一個極端困難的多目標折衷

- Synchrotron Radiation integrals:

$$I_1 = \oint \frac{\eta_x}{\rho_x} ds \qquad I_3 = \oint \frac{1}{|\rho_x^3|} ds$$

$$I_2 = \oint \frac{1}{\rho_x^2} ds \qquad I_4 = \oint 2\frac{\eta_x k}{\rho_x} ds$$

$$I_5 = \oint \frac{\mathcal{H}_x}{|\rho_x^3|} ds$$

- Energy spread:

$$\sigma_E^2 = C_q \frac{\gamma^2 I_3}{2I_2 + I_4}$$

- Equilibrium emittance:

$$\epsilon_x = C_q \frac{\gamma^2 I_5}{I_2 - I_4} \propto \frac{E^2}{N_{Dipole}^3} \quad \propto E^2 \theta^3$$

$$\mathcal{H} = \beta_x \eta_x'^2 + 2\alpha_x \eta_x \eta_x' + \gamma_x \eta_x^2$$

Coherence fraction:
phase space matching

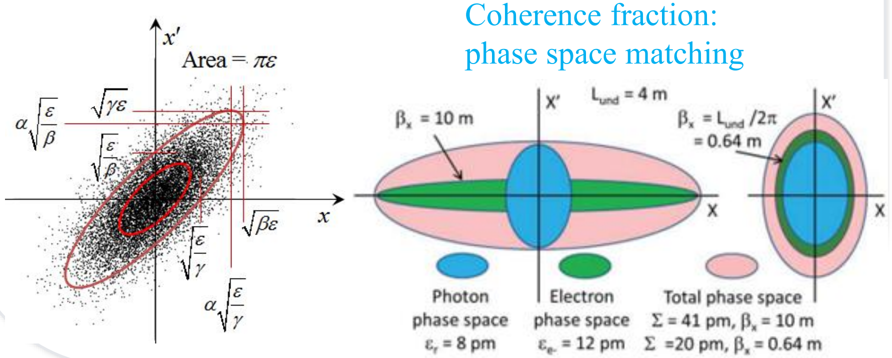

Ref: , A. Streun, PSI, Pushing the limits of storage ring light sources, UKSR50 workshop, June 26-29, 2018

Electron Motion in an Undulator

$B_y = B_0 \sin(kz)$, where $k = 2\pi/\lambda_0$ and λ_0 is the insertion device period length.

$$\ddot{x} = \frac{e}{\gamma m}\left(-\dot{z}B_y\right) \qquad \ddot{z} = \frac{e}{\gamma m}\left(\dot{x}B_y\right)$$

$$\dot{x} = \frac{eB_o}{\gamma m}\frac{\cos(kz)}{k} \qquad \beta_x = \dot{x}/c = \frac{K}{\gamma}\cos(kz)$$

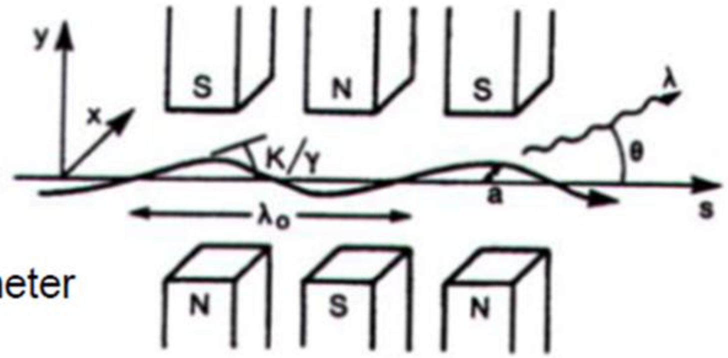

where the dimensionless undulator or deflection parameter is defined as follows:

$$K = \frac{eB_o\lambda_o}{2\pi mc} = 0.934 B_o[T]\lambda_o[cm]$$

$$\beta_x^2 + \beta_z^2 = \beta^2 \quad (= \text{constant})$$

$$\beta_z \cong \beta\left(1 - \frac{K^2}{4\gamma^2} - \frac{K^2}{4\gamma^2}\cos 2kz\right)$$

First integral field ∫Bds=0 (x'=0) & Second integral field ∫(∫ Bds')ds=0 (x=0)

The average velocity along the z-axis is thus: $\bar{\beta} \cong \beta\left(1 - \frac{K^2}{4\gamma^2}\right) \cong 1 - \frac{1}{2\gamma^2} - \frac{K^2}{4\gamma^2}$

We will only consider cases in which $K/\gamma << 1$ and so we can write to a good approximation that

$z = \bar{\beta}ct$ and $kz = \Omega t$ where $\Omega = 2\pi\bar{\beta}c/\lambda_o$. We have electron angle then:

$\dot{x} = \frac{K}{\gamma}c\cos(\Omega t)$ which can be integrated directly to give e-trajectory: $x = \frac{K}{\gamma}\frac{c}{\Omega}\sin(\Omega t)$

$$x' = \frac{K}{\gamma}\cos(\Omega t), \quad z = \bar{\beta}ct - \frac{K^2}{4\gamma^2}\frac{c}{2\Omega}\sin(2\Omega t), \quad \dot{z} = \bar{\beta}c - \frac{K^2}{4\gamma^2}c\cos(2\Omega t).$$

由運動方程式

$$\frac{d\vec{p}}{dt} = -e\,\vec{v} \times \vec{B}$$

得到橫向速度

$$\dot{x} = \frac{eB_0}{\gamma mk}\cos(kz)$$

因為總速度近似守恆：$\beta_x^2 + \beta_z^2 = \beta^2$

代入 β_x 後展開（到 K^2 階）：

$$\beta_z \simeq \beta\left(1 - \frac{K^2}{4\gamma^2} - \frac{K^2}{4\gamma^2}\cos 2kz\right)$$

平均縱向速度,對一個 undulator 週期取平均：

$$\bar{\beta}_z \simeq 1 - \frac{1}{2\gamma^2} - \frac{K^2}{4\gamma^2}$$

https://cds.cern.ch/record/362891/files/CERN-98-04.pdf

Insertion Devices: Undulators and Wigglers. Richard P. Walker, p131, Synchrotron Radiation and Free Electron Laser, 1996, CAS, CERN Accelerator School

Undulator Coherent Radiation:共振波長

In the time it takes the electron to move through one period length from point A to an equivalent point B ($\lambda_o / \bar{\beta} c$) the wavefront from A has advanced by a distance $\lambda_o / \bar{\beta}$ and hence is ahead of the radiation emitted at point B by a distance *d* where:

$$d = \frac{\lambda_o}{\bar{\beta}} - \lambda_o \cos\theta$$

and where *θ* is the angle of emission with respect to the electron beam axis. When this distance is equal to an integral number, *n*, of radiation wavelength there is constructive interference of the radiation from successive poles:

$$\frac{\lambda_o}{\bar{\beta}} - \lambda_o \cos\theta = n\lambda$$

Inserting the expression for the average electron velocity:

$$\frac{1}{\bar{\beta}} \cong 1 + \frac{1}{2\gamma^2} + \frac{K^2}{4\gamma^2}$$

results in the following interference condition:

$$\lambda = \frac{\lambda_0}{2n\gamma^2}\left(1 + \frac{K^2}{2} + \theta^2\gamma^2\right)$$

https://cds.cern.ch/record/362891/files/CERN-98-04.pdf

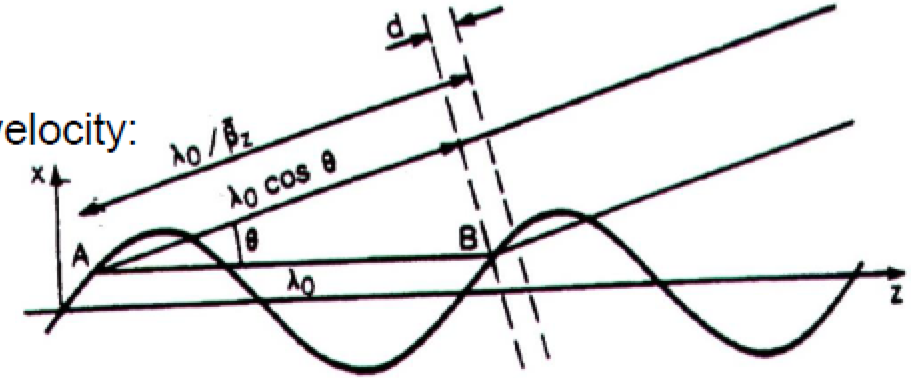

$K >> 1$ wiggler, $K \approx 1$ undulator,

$$K = \frac{eB_0\lambda_0}{2\pi mc} = 0.0934\, B_0[T]\, \lambda_0[mm]$$

電子從A點經過一個週期到B點,從A 點發出的電磁波波前已經前進了距離

$$\frac{\lambda_0}{\bar{\beta}}$$

因此相較於在 B 點所發射的輻射，其波前領先了一段距離 d：

$$d = \frac{\lambda_0}{\bar{\beta}} - \lambda_0 \cos\theta$$

其中 θ 為輻射相對於電子束軸線的發射角度

建設性干涉條件 $d = n\lambda$

代入並使用

$$\frac{1}{\bar{\beta}} \simeq 1 + \frac{1}{2\gamma^2} + \frac{K^2}{4\gamma^2}$$

即可得到以下的共振條件：

$$\lambda = \frac{\lambda_0}{2n\gamma^2}\left(1 + \frac{K^2}{2} + \theta^2\gamma^2\right)$$

Insertion Devices: Undulators and Wigglers. Richard P. Walker, p131, Synchrotron Radiation and Free Electron Laser, 1996, CAS, CERN Accelerator School

Principle of Free Electron Laser (FEL)

SASE：由 shot-noise 起始；Self-seeding：頻譜收斂；Seeded：全時間相干與可控上轉頻

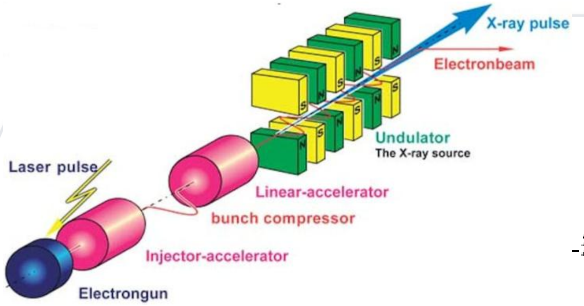

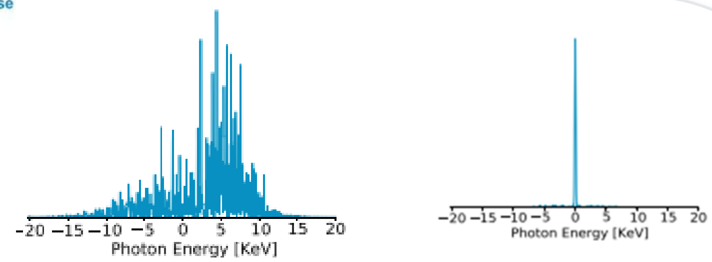

FELs produce coherent light by passing a beam of relativistic electrons through a periodic magnetic structure called an undulator or wiggler. The alternating magnetic fields of the undulator force the electron bunches to follow a sinusoidal path, causing them to emit synchrotron radiation. The key aspects of FEL operation include:

■**Electron Beam**: A high-energy, relativistic electron beam is produced by a linear accelerator (linac).

■**Undulator**: The electron beam passes through the undulator, which consists of alternating magnetic fields that induce transverse oscillations in the electrons.

■**Micro-bunching**: The emitted radiation interacts with the electron beam, leading to the formation of micro-bunches, where electrons bunch together at the radiation wavelength.

■**Amplification**: The micro-bunched electrons radiate coherently, amplifying the emitted light in a process called Self-Amplified Spontaneous Emission (SASE).

$$K = \frac{eB_0\lambda_0}{2\pi mc} = 0.0934\, B_0[T]\, \lambda_0[mm]$$

Ref: https://www.psi.ch/en/swissfel/how-it-works

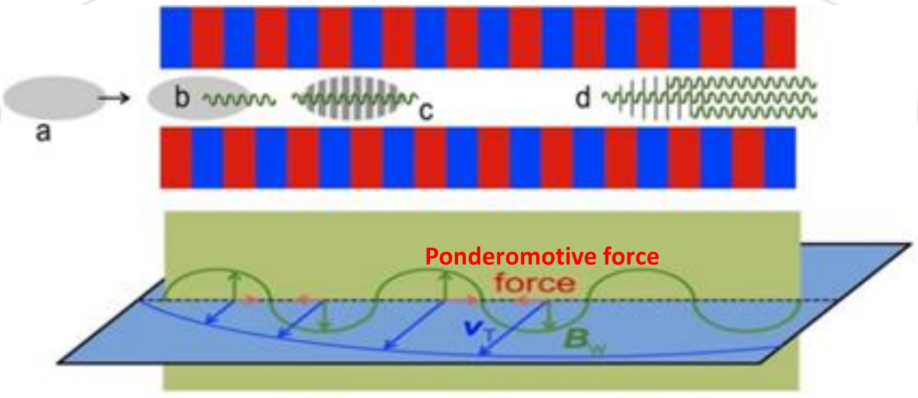

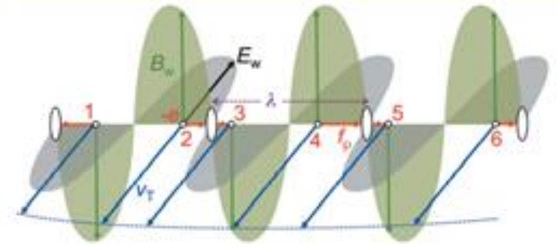

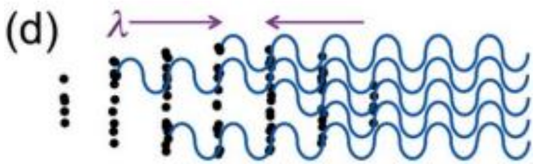

$$\lambda = \frac{\lambda_0}{2n\gamma^2}\left(1 + \frac{K^2}{2} + \theta^2\gamma^2\right)$$

The magnetic field B_w (green) of radiation and the electron transverse velocity v_T (blue) cause the Lorentz forces (red). These slightly shift the positions of the electrons along the bunch until they reach one of the wave nodes. The slices are created at every other node, so their spacing equals one wavelength of radiation.

Microbunching

SASE：由 shot-noise 起始；Self-seeding：頻譜收斂；Seeded：全時間相干與可控上轉頻

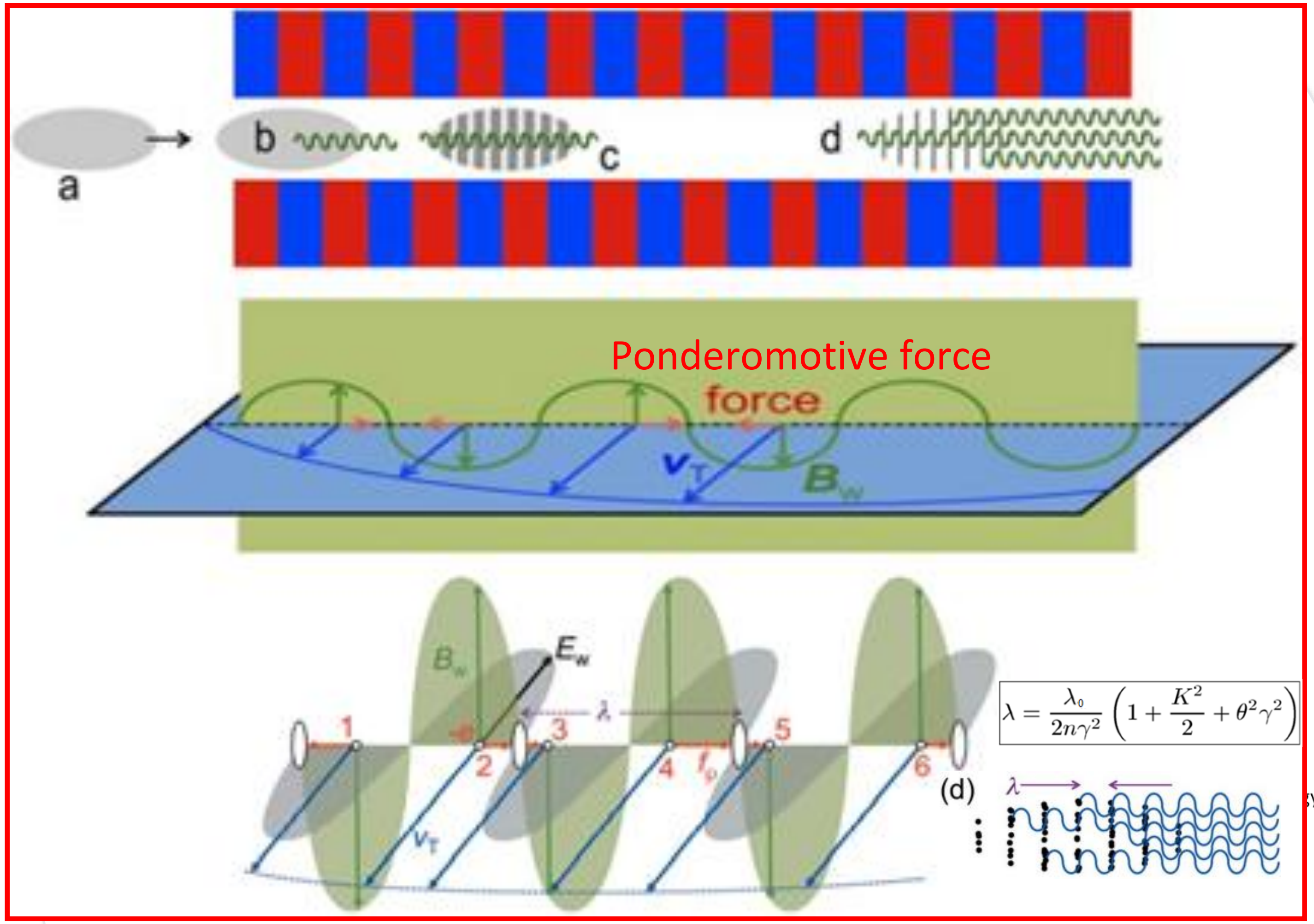

Planner Undulator cause electron beam oscillation in x direction: V_T

Ref: Synchrotron radiation and X-ray free-electron lasers (X-FELs) explained to all users, active and potential, Yeukuang Hwua, and Giorgio Margaritondod, 2021, JSR

■Differential equations of the low-gain FEL

$$\frac{d\psi}{dt} = 2k_u c\,\eta \qquad \frac{d\eta}{dt} = -\frac{eE_0K}{2m_e c\gamma_r^2}\cos\psi \qquad \eta = \frac{\gamma - \gamma_r}{\gamma_r}$$

$$\ddot{\psi} + \Omega^2\cos\psi = 0 \quad \text{with} \quad \Omega^2 = \frac{eE_0Kk_u}{m_e\gamma_r^2}$$

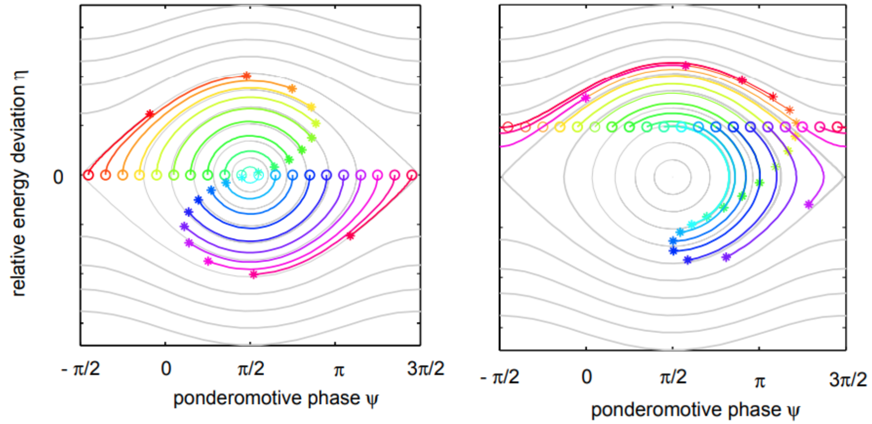

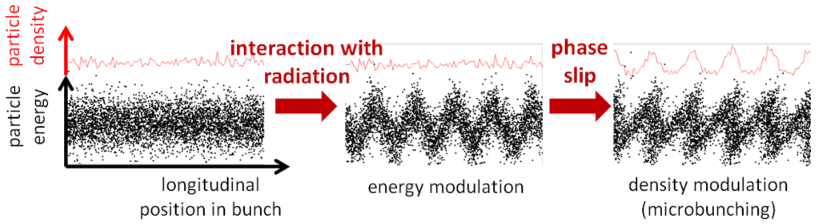

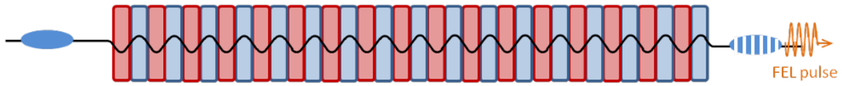

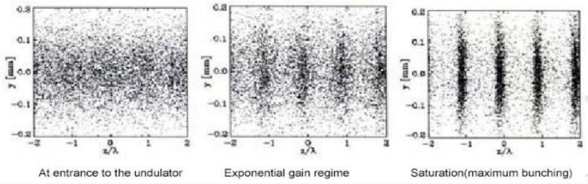

從 SASE 到 Seeded：相干性與頻譜的差異

SASE：由 shot-noise 起始；Self-seeding：頻譜收斂；Seeded：全時間相干與可控上轉頻

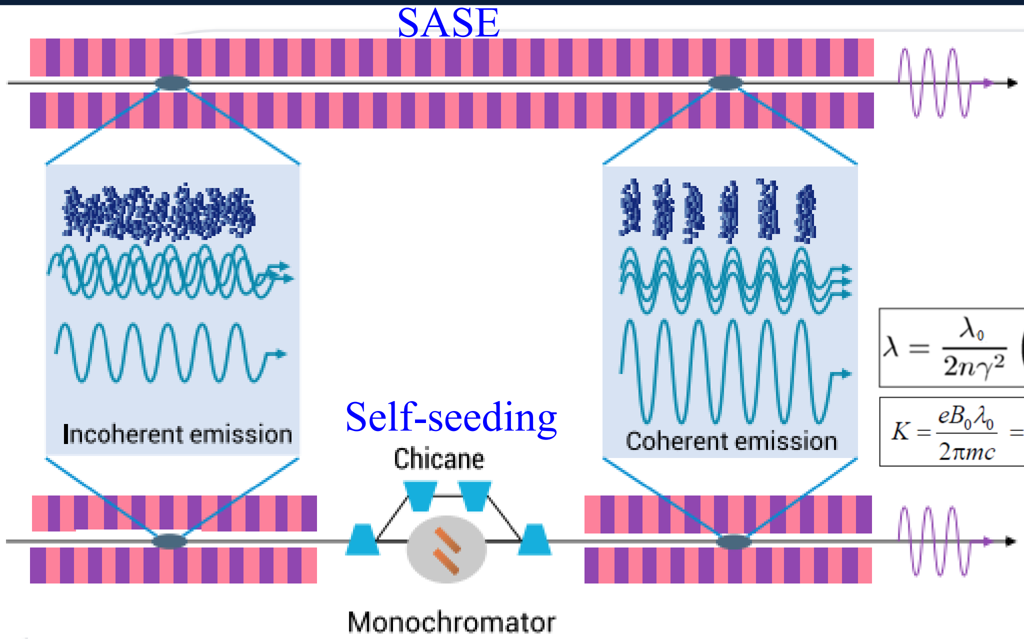

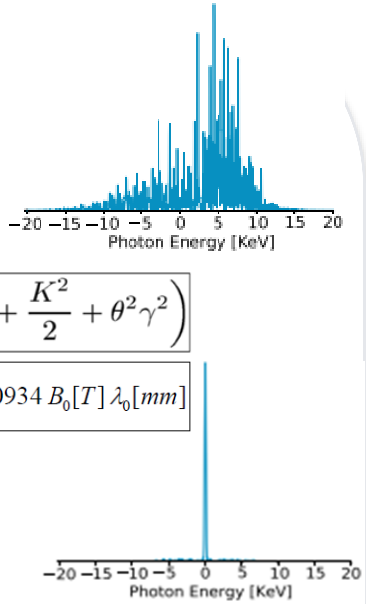

$$\lambda = \frac{\lambda_0}{2n\gamma^2}\left(1 + \frac{K^2}{2} + \theta^2\gamma^2\right)$$

$$K = \frac{eB_0\lambda_0}{2\pi mc} = 0.0934\, B_0[T]\, \lambda_0[mm]$$

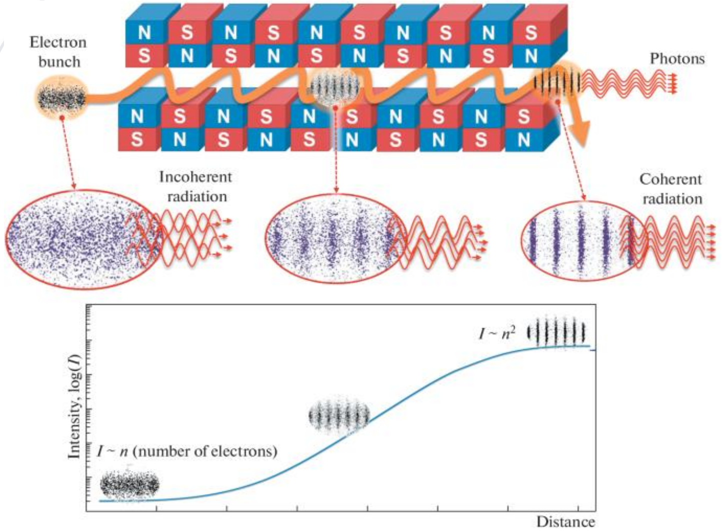

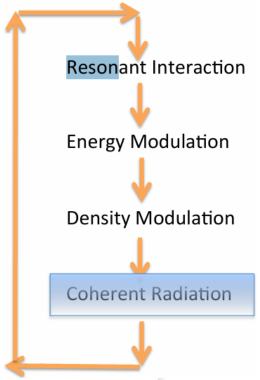

- **SASE** starts from the intrinsic shot noise of the electron beam, leading to spontaneous emission that is amplified as it travels through the undulator. SASE FELs provide excellent transverse coherence but relatively poor temporal coherence.
- **Self-seeding**: part of the FEL output is used as a seed for subsequent amplification stages, enhancing temporal coherence and narrowing the bandwidth.

重點比較

- SASE：容易啟振、橫向相干佳；但時間相干差、shot-to-shot 頻譜抖動
- Self-seeding：以 monochromator/晶體濾波再播種 — 頻譜變窄
- Seeded（HGHG/EEHG/PEHG）：外部種子決定相位 — 最佳時間相干與可重複性

Ref: Features and futures of X-ray free-electron lasers, Nanshun Huang, et. al. The innovation, 2021

Magnetic Bunch Compression

Chicane R_{56}

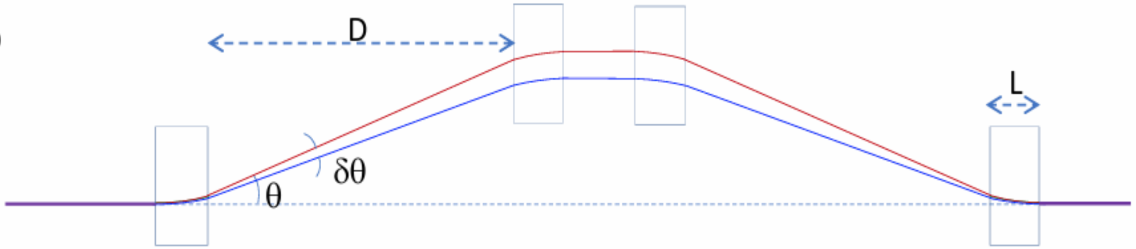

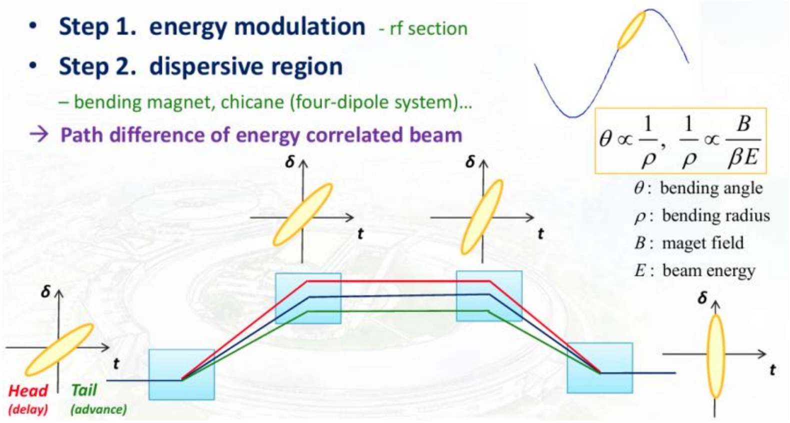

At E_0, the beam follows the red path with an extra pathlength relative to the straight path (dashed) as given by

$$l = \left(\frac{2}{3}L + D\right)\theta^2$$

If we raise the beam energy to $E_0 + \delta E$, the beam follows a slightly shorter path (blue) with an extra pathlength

$$l + \delta l = \left(\frac{2}{3}L + D\right)(\theta - \delta\theta)^2 \approx \left(\frac{2}{3}L + D\right)(\theta^2 - 2\theta\delta\theta)$$

Relative energy change

$$\delta = \frac{\delta E}{E_0}$$

Relative angle change

$$\frac{\delta\theta}{\theta} = -\delta$$

Pathlength change relative to δ

$$R_{56} = -2\left(\frac{2}{3}L + D\right)\theta$$

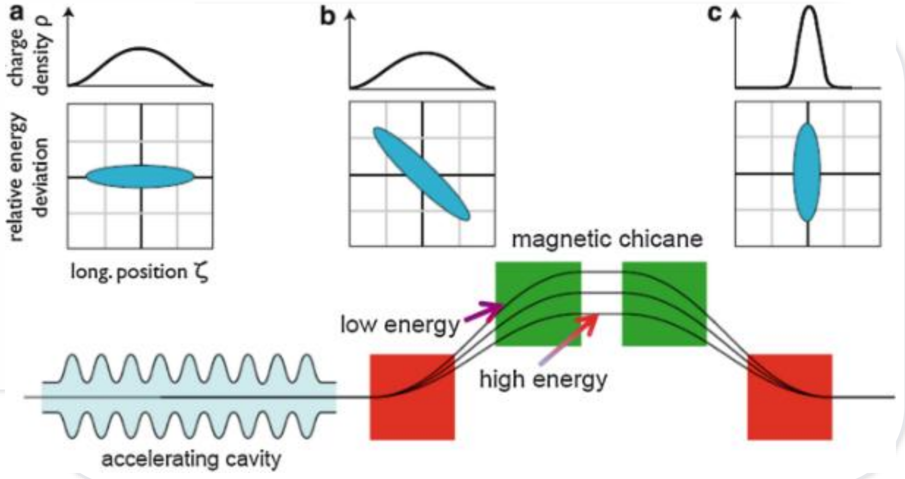

Seeded FEL 三種代表機制：HGHG / EEHG / PEHG

Why need harmonic generation?

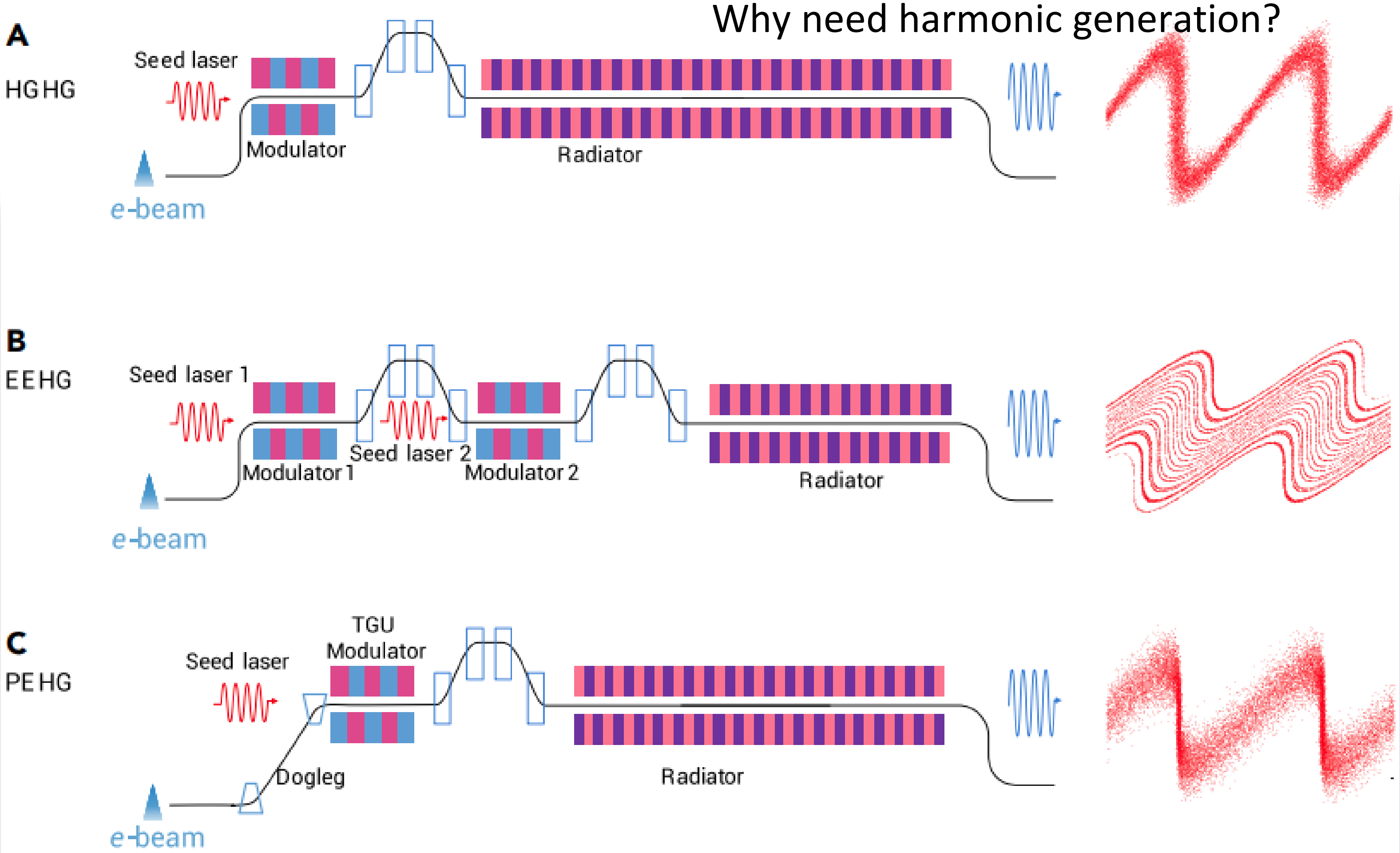

HGHG: High gain Harmonic Generation
EEHG: Echo-Enabled Harmonic Generation
PEHG: Phase-Enhanced Harmonic Generation
TGU: Transverse Gradient Undulator

$$\lambda = \frac{\lambda_0}{2n\gamma^2}\left(1 + \frac{K^2}{2} + \theta^2\gamma^2\right)$$

$$K = \frac{eB_0\lambda_0}{2\pi mc} = 0.0934\, B_0[T]\, \lambda_0[mm]$$

Ref: Features and futures of X-ray free-electron lasers, Nanshun Huang, et. al. The innovation, 2021

HGHG:

Core idea: single energy modulation → chicane bunching, Harmonic reach: low (≤10). Complexity: low. Key trade-off: simple and robust, but wavelength-limited

EEHG :

Core idea: two energy modulations with echo interference. Harmonic reach: very high (50–100+). Complexity: high. Key trade-off: highest harmonic reach, highly sensitive to beam quality

PEHG:

Core idea: phase merging via dogleg + TGU. Harmonic reach: high (30–100). Complexity: very high. Key trade-off: relaxed energy-spread constraint at the cost of complex hardware

Common features:

Seeded operation. Full temporal coherence. Radiator-based FEL gain

Seeded FEL 三種代表機制：HGHG / EEHG / PEHG

HGHG（高增益諧波產生）:在 modulator undulator 讓種子雷射與電子束作用，先在縱向產生正弦型能量調制；接著通過色散段（chicane, *R*56）把能量調制轉成密度調制（bunching），在第 *n* 次諧波形成可被 radiator 放大的微聚束，輸出具完全時間相干的輻射。但因高諧波需要較大調制與色散，對能量散佈與非線性展寬敏感，單級通常諧波數受限。

EEHG（回聲式諧波產生）:在兩個 modulator 與兩個色散段中，先用強色散把相空間剪切成細條紋結構，再經第二次調制與較弱色散觸發回聲干涉，從較溫和的能量調制產生極高諧波的密度調制，因此可把相干種子推進到更短波段；代價是對束流能散、CSR/ISR 擴散與相位抖動容忍度較低。
https://journals.aps.org/prab/pdf/10.1103/PhysRevSTAB.12.030702

PEHG（相位合併增強 HGHG）: 利用 dogleg 先建立橫向色散 $x=\eta\delta$，再用 TGU（橫向梯度 undulator） 使不同能量粒子在橫向上經歷不同磁場、但在縱向相位上被合併（phase merging）到近似同一相位，等效降低能散對 bunching 的破壞，因而具高諧波潛力；然而需要精密橫向-縱向耦合設計與 TGU 工程實現。
https://arxiv.org/pdf/1312.2823

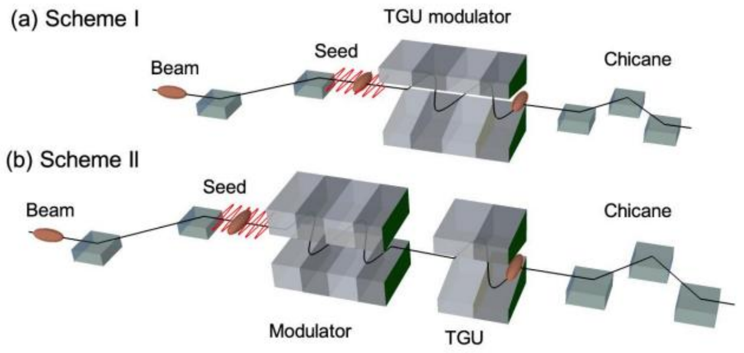

Figure 1. (a) Original PEHG scheme with a TGU modulator for energy modulation and phase-merging simultaneously; (b) An PEHG variant with a normal modulator for energy modulation and a TGU for introducing the phase-merging effect.

Facilities of Free Electron Laser around the World

FEL 的關鍵能力來自電子與輻射場的自洽耦合所引發的微束化與電子間相位鎖定，進而形成 Ne^2 等級的相干增益與近單色雷射輸出。此一運作機制需要極低能量散佈、短束團或高峰值電流、長 undulator 以及嚴格的同步與抖動控制，通常必須建立在直線加速器的單通過高增益架構之上

Ref: Features and futures of X-ray free-electron lasers, Nanshun Huang, et. al. The innovation, 2021

左邊這條趨勢軸線反映三個關鍵演進方向：

- **由低能至高能光子能段**（soft X-ray → hard X-ray）
- **由低重複率至高重複率（quasi-CW / CW）**
- **由常導（NC）直線加速器走向超導（SC）直線加速器**

■**FLASH**: 1st soft X-ray FEL in the word

■**FERMI**: 1st seeded soft X-ray FEL

■**LCLS**: 1st hard X-ray FEL in the word

■ **SACLA:** A compact hard X-ray FEL

■ **PAL-XFEL: A** hard X-ray with femtosecond-scale timing jitter

■ **Eu-XFEL:** 1st MHz-repetition-rate hard X-ray FEL

■ **Swiss-FEL:** An ultra-compact hard X-ray FEL

■ **LCLS-II:** 1st quasi-CW high-repetition-rate XFEL

Facilities of Free Electron Laser around the World

	European XFEL	LCLS	LCLS-II, CuRF	LCLS-II, SCRF	SACLA	SwissFEL	PAL-XFEL	SHINE
Start of commissioning	2016	2009	2019	2020	2011	2016	2016	2025
Accelerator technology	Super-conducting	Normal-conducting	Normal-conducting	Super-conducting	Normal-conducting	Normal-conducting	Normal-conducting	Super-conducting
Length of the facility	3.4 km	3 km	3 km	3 km	0.75 km	0.74 km	1.1 km	

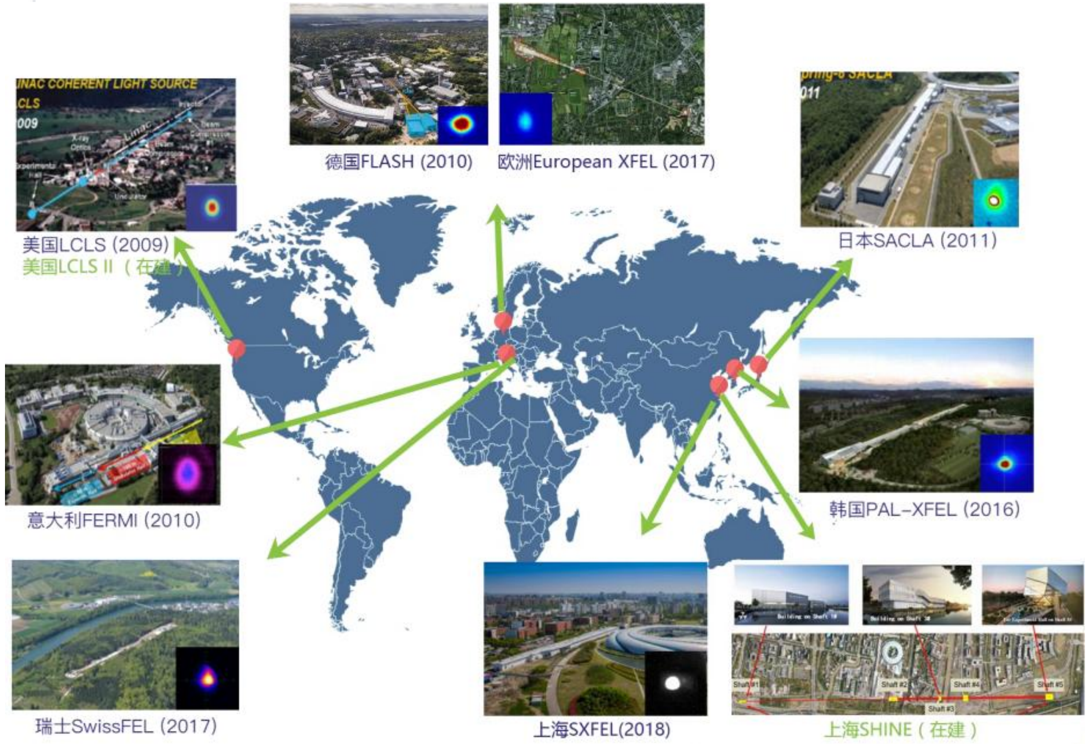

Parameter	NC	SC
Surface resistance (R_s)	$\propto f^{1/2}$	$\propto f^{2}$
Quality factor (Q)	$\propto f^{-1/2}$	$\propto f^{-2}$
Shunt impedance per unit length (r)	$\propto f^{1/2}$	$\propto f^{-1}$
r/Q	$\propto f$	
Longitudinal wakefield ($w_{//}$)	$\propto f^{2}$	
Transverse wakefield ($w_{\perp}$)	$\propto f^{3}$	

在高重複率、高平均電流 FEL 中，wakefield 直接影響：能量散佈成長微束化品質增益長度與飽和行為多束團不穩定性超導系統可在較低加速梯度與較大腔孔徑下運轉，有利於抑制 wakefield 與累積阻抗效應

https://www.xfel.eu/facility/comparison/index_eng.html

Facilities of Free Electron Laser around the World

Table 1. Major parameters for worldwide X-ray FEL facilities

Facility	Beam energy (GeV)	Photon energy (eV)	Repetition rate (Hz)	Pulse duration (FWHM) (fs)
FLASH	0.35–1.25	14–620	4×10^3 to 10^6	10–200
LCLS	2.5–16.9	280–12,800	120	5–400
SACLA	5.1–8.5	4,000–20,000	60	2–10
FERMI	1–1.5	20–310	50	30–100
PAL-XFEL	3.5–10	275–20,000	60	5–100
SwissFEL	2.1–5.8	250–1,240	100	1–20
European XFEL	8.5–17.5	240–25,000	2.7×10^4	3–150
SXFEL	1.0–1.6	124–1,000	50	30–1,000
LCLS-II (HE)	4–15	200–25,000	$120/10^6$	1–500
SHINE	8	400–25,000	10^6	3–600

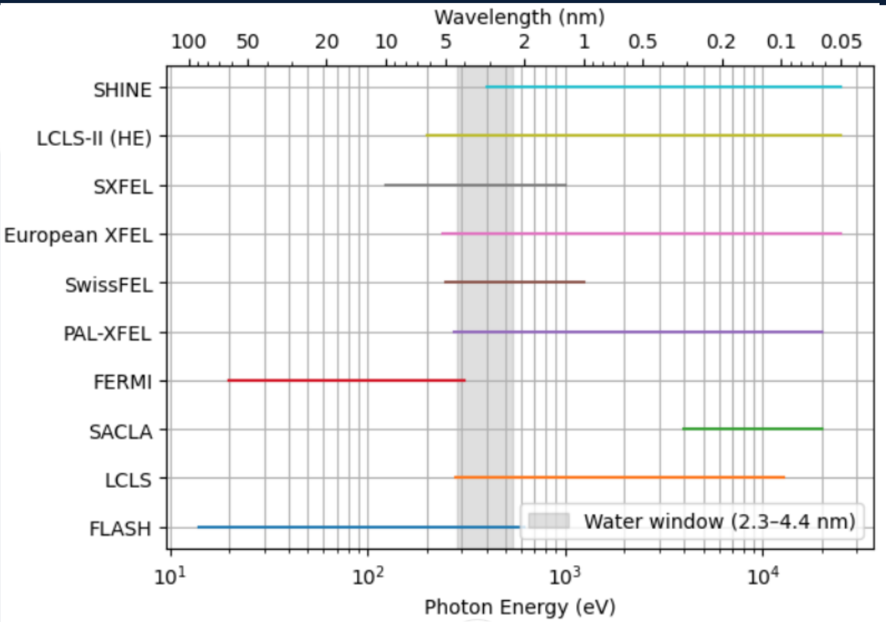

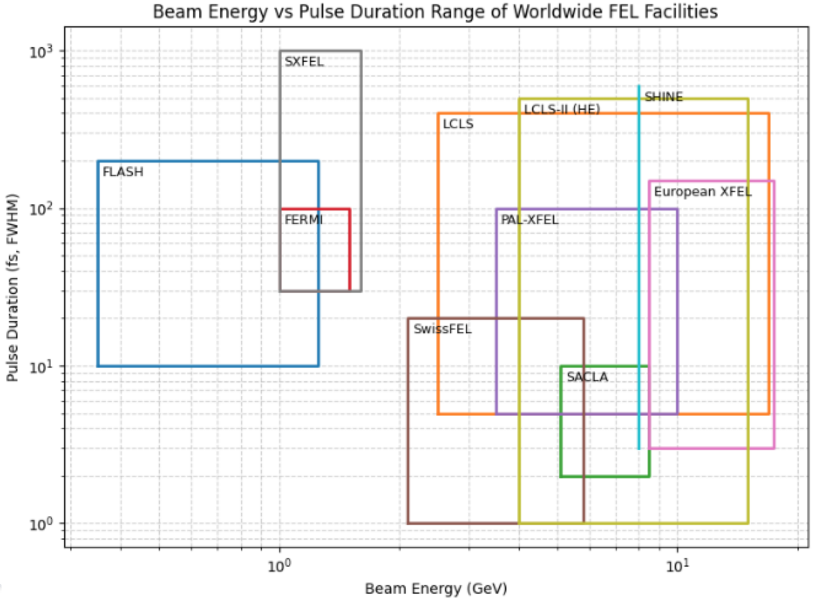

Water Window: 是一個獨特的光譜區域，在此軟 X 光的空間相干性、生物樣品的天然吸收對比，以及超快時間尺度的動力學量測條件得以同時實現，使其成為相干生物成像與動態研究的關鍵能段。

SwissFEL：

目標：

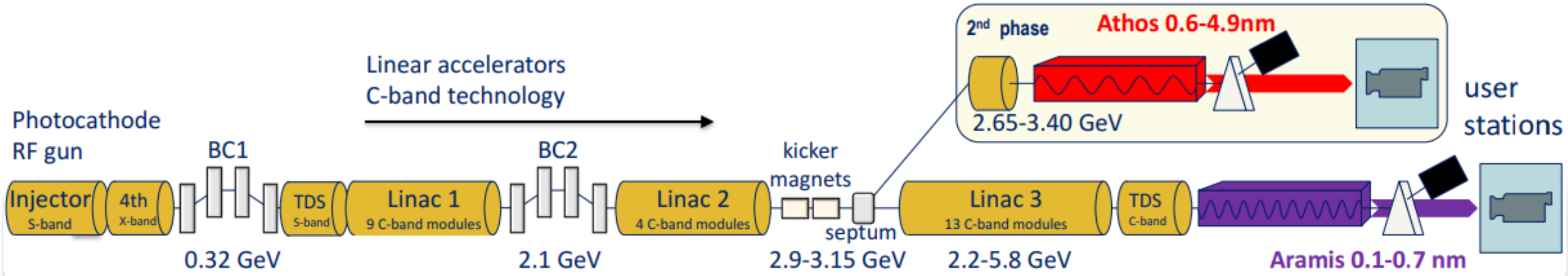

1 電子槍與注入器（Injector）

•Photocathode RF gun（S-band）

用雷射打在光陰極上產生電子束，是整個系統的起點。

•X-band linearizer（4th X-band）

用來修正縱向相空間非線性，讓後續壓縮更有效。

•出口能量約 **0.32 GeV**

2 束團壓縮與前段直線加速

•BC1、BC2（Bunch Compressor）

利用 RF chirp + 磁壓縮，將 bunch 壓短以提升峰值電流。

•Linac 1（C-band）+ Linac 2（C-band）

Linac 1：9 個 C-band module

Linac 2：4 個 C-band module

•能量提升到約 **2.1 GeV → 2.9–3.15 GeV**

3 分流與第三段直線加速（Linac 3）

•Kicker magnets + Septum

決定電子束要送往哪一條 FEL 線站

•Linac 3（13 個 C-band module）

最終能量範圍：**2.2–5.8 GeV**

4 兩條 FEL 線站

•Aramis（0.1–0.7 nm，硬 X-ray）

高能量

短波長

•Athos（0.6–4.9 nm，軟 X-ray）

第二期新增

專為先進光學操控與相干實驗設計

這裡就是 **SASE / seeded FEL** 發生的地方

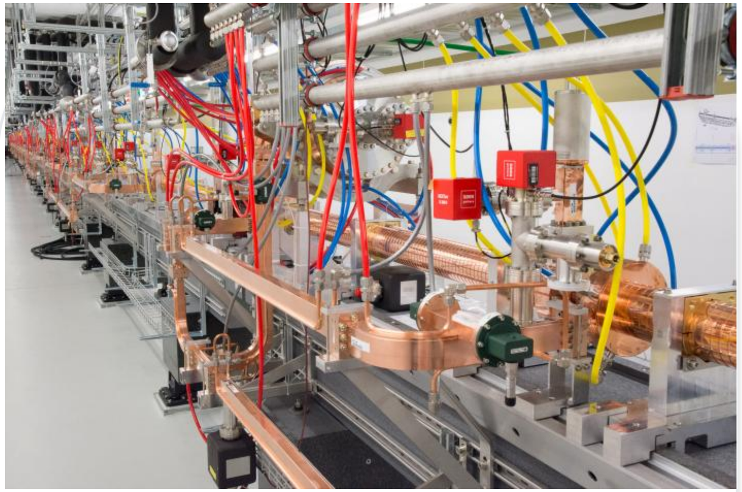

真實的 SwissFEL C-band 加速器模組一隅:

•銅製 RF 結構（加速腔）

•大量 水冷管線（黃色、藍色）

•RF coupler、真空元件

•精密的 機械對準結構

SwissFEL: an undulator period of 15 mm, a K-value of 1.2 and an energy of 5.8 GeV (γ = 11000) would give 1 Å radiation

$$\lambda = \frac{\lambda_0}{2n\gamma^2}\left(1 + \frac{K^2}{2} + \theta^2\gamma^2\right)$$

Accelerator Layout for Free Electron Laser (FEL)

Layouts of S-band (top), C-band (middle), and X-band (bottom) based XFEL driving linacs

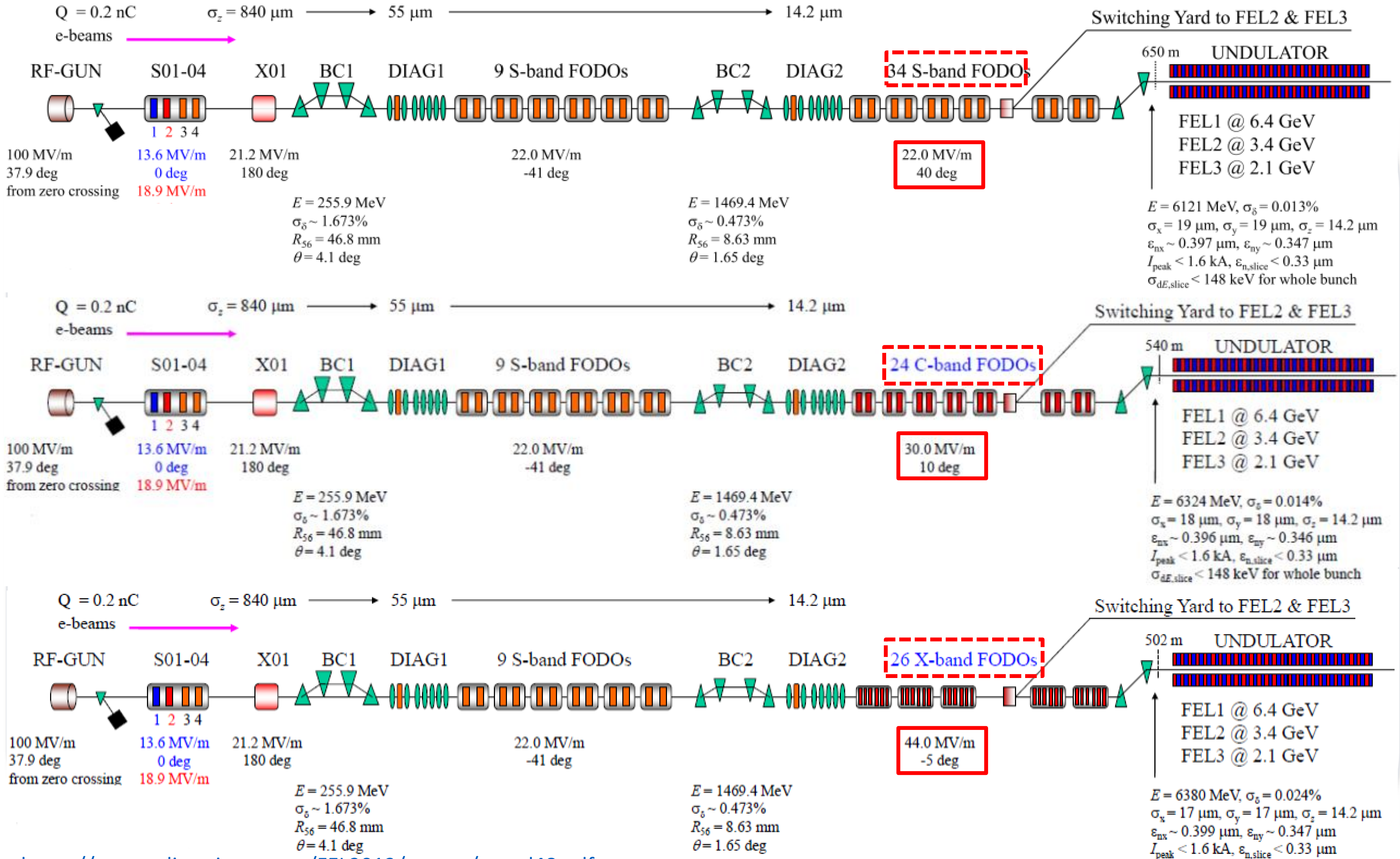

https://proceedings.jacow.org/FEL2012/papers/mopd48.pdf

Ref: FEL2012, Nara, Japan, MOPD48, Yujong Kim, et. al

■ S-band (~3 GHz)
- Lowest RF frequency
- Moderate gradient (~20–22 MV/m)
- Requires **longest linac** for a given beam energy

■ C-band (~6 GHz)
- Intermediate frequency
- Higher gradient (~30 MV/m)
- Enables **significantly shorter linac** than S-band

■ X-band (~12 GHz)
- Highest frequency
- Highest gradient (~40–45 MV/m)
- **Shortest linac**, most compact facility

Steady-State Micro-Bunching (SSMB):
Phase I & II @ MLS, phase III: dedicated storage ring

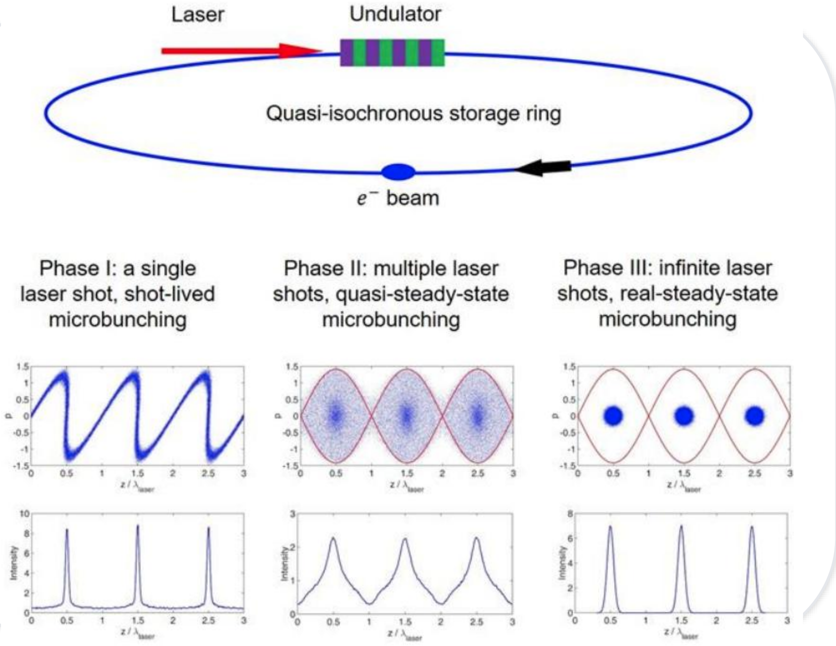

以實驗方式驗證了穩態微束團化 SSMB 的關鍵物理機制。研究團隊選用準等時的低能量儲存環，透過雷射與波蕩器交互作用，先在電子束上施加能量調制，再利用環中縱向相位滑移將能量調制轉換成密度調制，使束流在雷射波長尺度上形成明顯的micro-bunching結構。最重要的是，他們觀察到電子束在繞行一圈之後仍能維持與雷射相位相關的微結構，顯示「逐圈相位記憶能在真實儲存環條件下實現。為了證明輻射確實來自相干增強，論文以多種觀測指標建立因果鏈。包含相干輻射強度隨束流電荷呈現接近平方的成長關係，頻譜顯示出相對窄的帶寬，且只有在雷射調制條件成立時才會出現顯著增強。這些結果共同支持微束團化已在束流中形成，並能有效轉化為相干輻射輸出。作者同時強調，本研究展示的是 SSMB 的核心機制與可行性基礎，而非完整的 SSMB 光源系統，距離更短波長如 EUV 的實用化仍受限於準等時磁格的相位容限，量子擴散與集體效應，以及長期相位鎖定雷射系統等挑戰。

Experimental demonstration of the mechanism of steady-state microbunching

MLS:
Metrology
Light Source,
Berlin

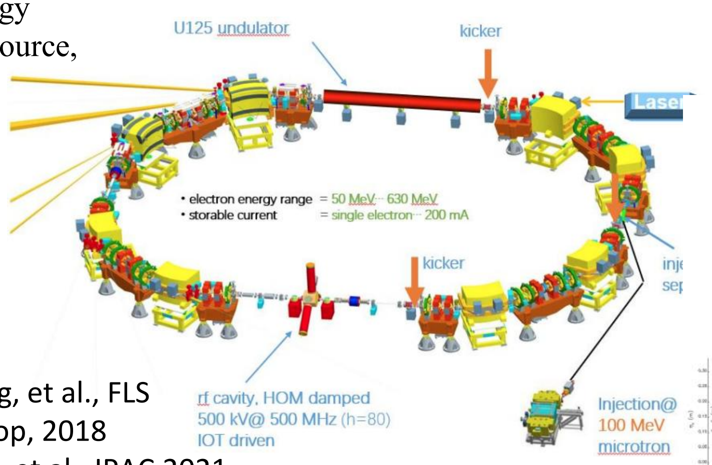

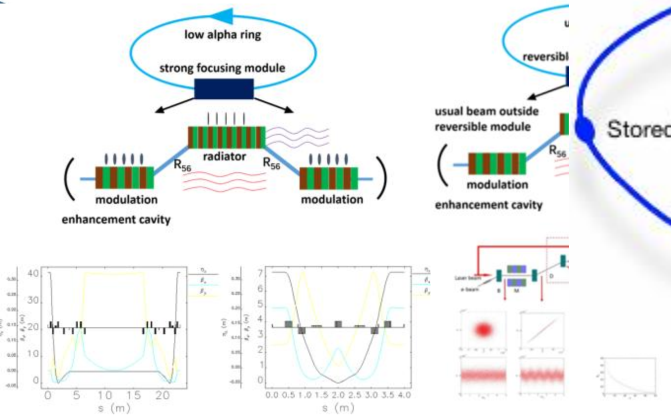

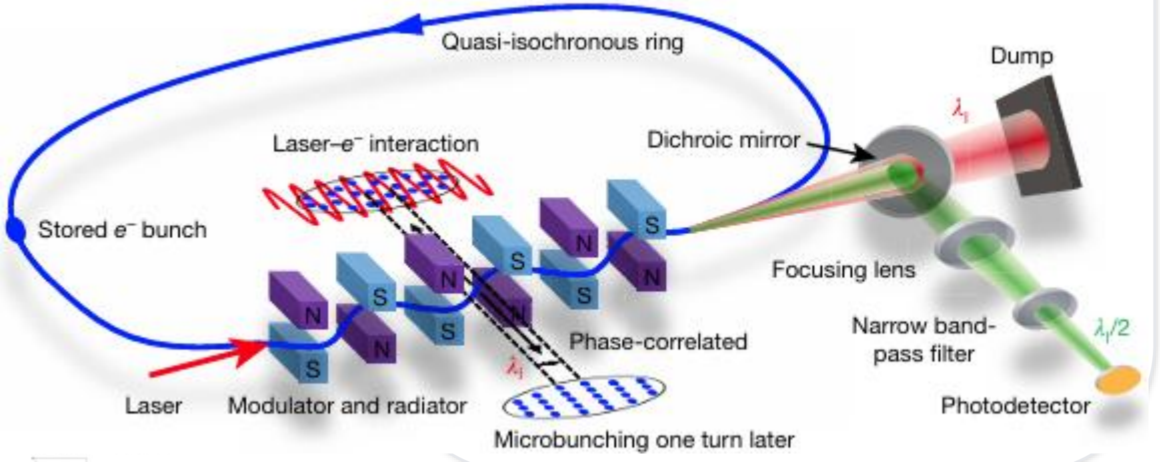

C.X. Tang, et al., FLS Workshop, 2018
J. Feikes, et al., IPAC 2021

Energy Recover LINAC (ERL)

共同目標：

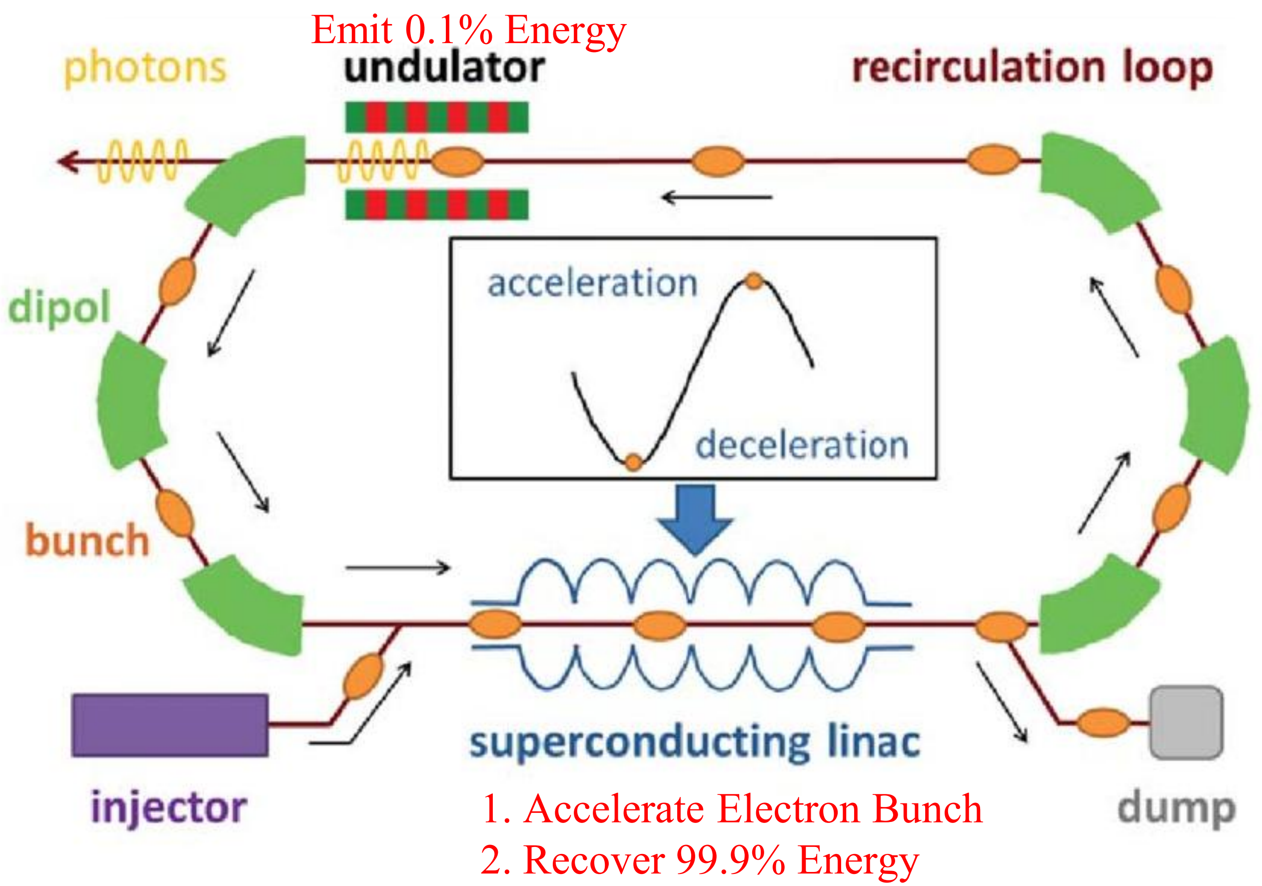

能量回收直線加速器（ERL）是一種以超導直線加速器（SCRF linac）為核心的加速器架構。電子束團首先由注入器產生，經 linac 加速至高能量後通過波蕩器產生同步輻射，隨後並非直接送往束流傾倒，而是經由回旋輸運線重新注入同一條 linac，並在 RF 相位反轉（π phase shift）下進行減速，將電子束所攜帶的動能回饋至 RF 腔體。

EUV-FEL Light Source for Future Lithography

14th International Particle Accelerator Conference,Venice, Italy JACoW Publishing
ISBN: 978-3-95450-231-8 ISSN: 2673-5490 doi: 10.18429/JACoW-IPAC2023-THPM123

EUV-FEL LIGHT SOURCE FOR FUTURE LITHOGRAPHY

N. Nakamura†, R. Kato, H. Sakai, K. Tsuchiya, Y. Tanimoto, Y. Honda, T. Miyajima#, M. Shimada, T. Tanikawa, O. A. Tanaka, T. Obina, H. Kawata
High Energy Accelerator Research Organization (KEK), Tsukuba, Japan

本研究提出一套以能量回收直線加速器（ERL）為核心的高功率 EUV-FEL 光源構想，目標應用於次世代半導體微影（13.5 nm）。系統採用 500 kV DC 光陰極槍，在連續波（CW）模式下將電子束加速至 800 MeV、約 10 mA，經波蕩器產生高功率 EUV-FEL 後，再將束流送回主直線進行減速能量回收，可回收數 MW 等級功率，大幅降低壁插功率需求。
目前完整 EUV-FEL by ERL 尚未建成，作者以 KEK 的 compact ERL（cERL）作為 Proof oC 平台，進行低能量 IR-FEL / SASE 實驗，逐步驗證注入器亮度、能量回收穩定性與 FEL 增益等關鍵技術。

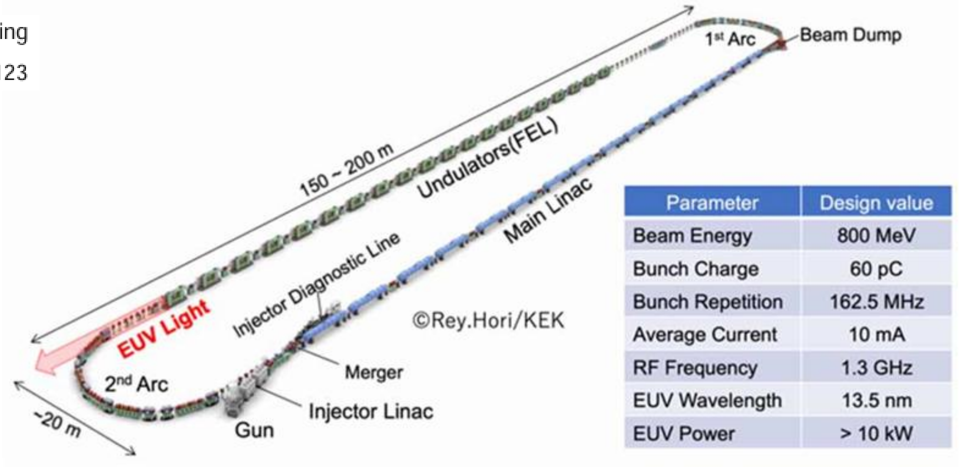

Parameter	Design value
Beam Energy	800 MeV
Bunch Charge	60 pC
Bunch Repetition	162.5 MHz
Average Current	10 mA
RF Frequency	1.3 GHz
EUV Wavelength	13.5 nm
EUV Power	> 10 kW

Figure 1: 3-D illustration and design parameters of the EUV-FEL light source based on ERL.

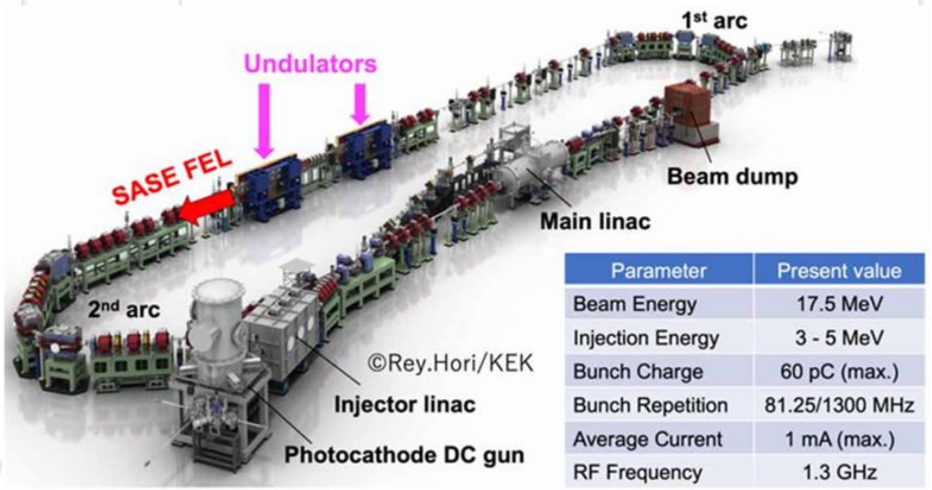

Parameter	Present value
Beam Energy	17.5 MeV
Injection Energy	3 - 5 MeV
Bunch Charge	60 pC (max.)
Bunch Repetition	81.25/1300 MHz
Average Current	1 mA (max.)
RF Frequency	1.3 GHz

Figure 5: Schematic of PoC of the EUV-FEL light source using the cERL and the cERL parameters.

Energy Recover LINAC (ERL) facilities around the world

目標：

Facility	Status	Layout / Topology	Primary Purpose	Key Capability
s-DALINAC (TU Darmstadt)	In operation; demonstrated one-turn and two-turn ERL	SRF linac + recirculation; 180° phase shift for deceleration	ERL operation and phase/efficiency studies	Superconducting multi-turn ERL operation
CBETA (Cornell)	Operational ERL test accelerator; multi-pass demonstrated	SRF linac + FFAG return loop; multi-energy transport	ERL optics and system integration R&D	Multi-energy, multi-pass ERL optics (FFAG)
MESA (Mainz)	Under construction / commissioning	Thrice-recirculating SRF ERL; multiple operation modes	Nuclear and particle physics user facility	User-oriented CW ERL operation
EIC Cooler (BNL)	Design and project development stage	High-brightness injector + ERL/recirculator + cooling section	Electron cooling for hadron beams	ERL applied to beam cooling
cERL (KEK)	Operational; mA-class fully energy-recovered beam	Compact ERL; high-voltage DC gun + SRF cavities	ERL core technology and application R&D	Injector brightness and low-loss energy recovery
BINP Recuperator / NovoFEL	Long-term user operation	Multi-turn ERL with multiple FELs on different orbits	THz / IR FEL user facility	High-average-power ERL-FEL
CEBAF (JLab)	Operational user facility	Two SRF linacs + five-pass recirculating linac	Nuclear physics beam delivery; ER methodology	High-energy multi-pass SRF linac
JLab FEL	Operational user FEL	ERL-driven FEL with energy recovery	High-average-power IR/THz FEL	Most mature ERL-FEL example
bERLinPro / SEALab (HZB)	Commissioning since 2024	SRF photoinjector-centered ERL platform	Next-generation ERL injector R&D	High-current SRF injector technology

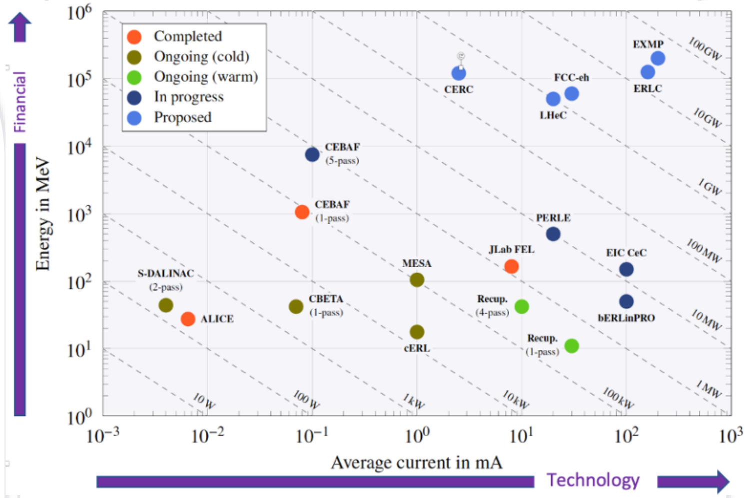

Laser Plasma Wakefield Accelerator

雷射電漿尾場加速器是一種利用超短、超高強度雷射脈衝在電漿中產生強電場，以實現超高加速梯度的新型加速技術。其核心概念是：雷射本身不直接加速電子，而是透過激發電漿尾場，讓電子在尾場中被加速。當一束飛秒等級的強雷射脈衝聚焦並射入氣體噴嘴（Gas Jet）後，氣體被瞬間電離形成電漿。雷射在電漿中傳播時，其龐德莫力（Ponderomotive force）會將電漿電子推離雷射路徑，使電子與離子發生空間分離。由於離子較重、幾乎不動，便在雷射後方形成一系列類似水波的電漿振盪結構（尾場）。在這些電漿尾場中，會出現極強的縱向加速電場（Acceleration field），其強度可達傳統射頻加速器的數百到上千倍。若電子束（Electron bunch）被正確注入到尾場的加速相位中，電子就能在極短距離內被迅速加速至高能量，形成高能電子束（Electron beam）。

由於其體積小、梯度高、潛在成本低，雷射電漿尾場加速器被視為下一代緊湊型加速器與未來先進光源（如小型自由電子雷射）的重要發展方向

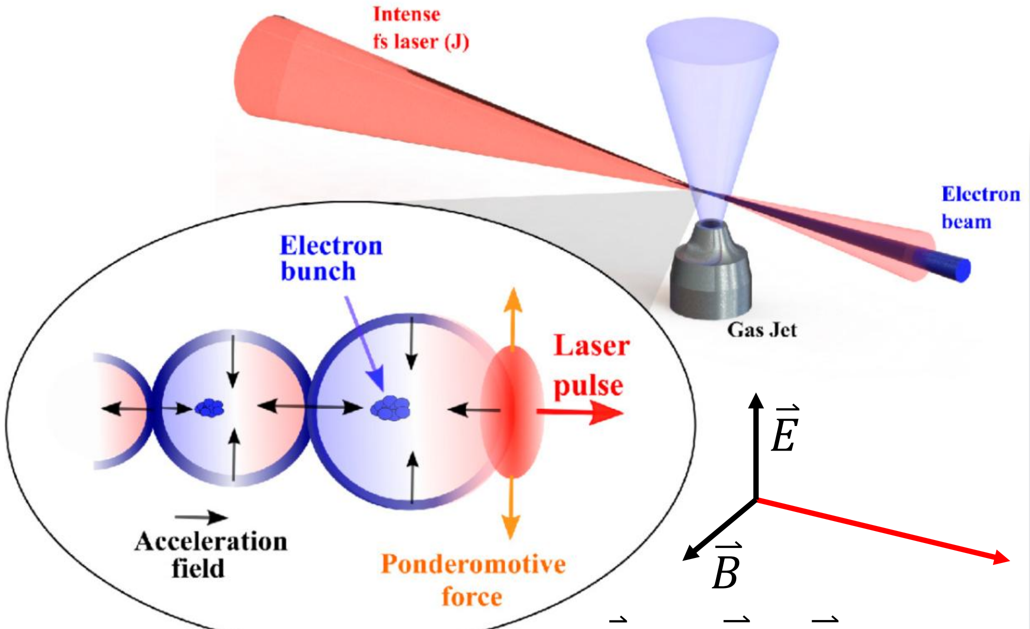

$$\vec{F} = q\vec{V} \times \vec{B}$$

紅色區域代表雷射脈衝（Laser pulse）
橘色箭頭表示龐德莫力
藍色結構為電漿電子密度調制形成的尾場
黑色箭頭表示加速電場方向

FEL driven by a compact laser plasma accelerator (SASE FEL, 27 nm)

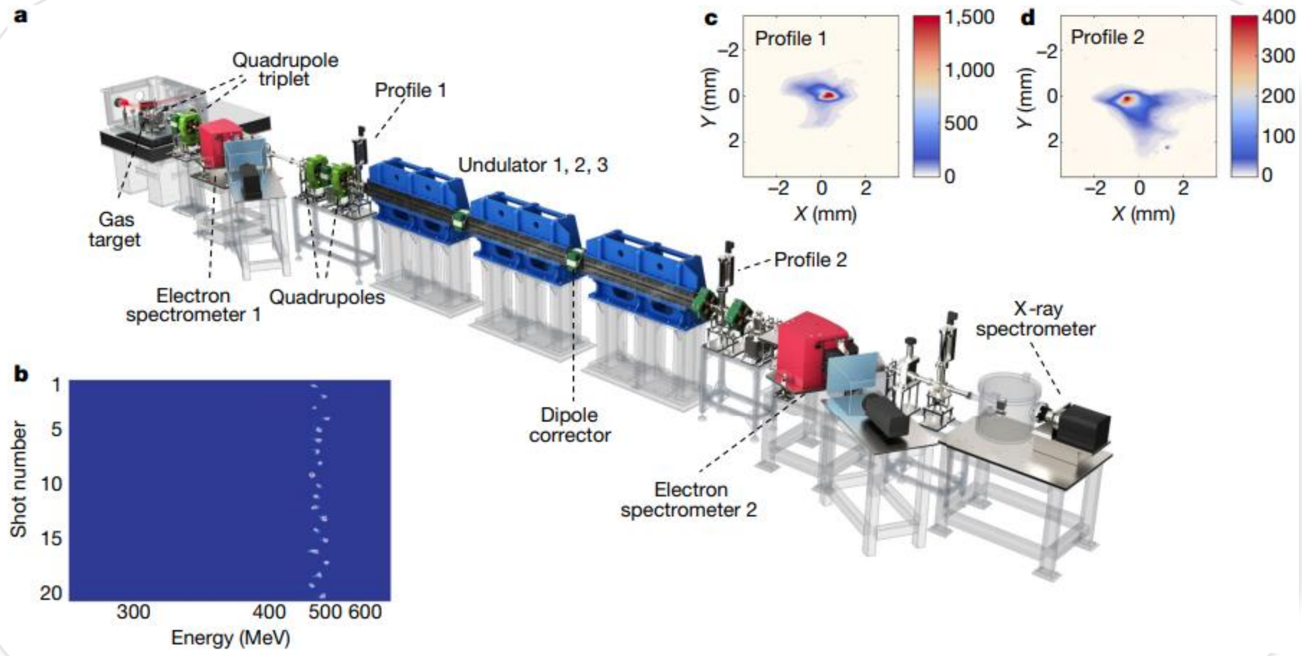

本研究首次在實驗上證實：雷射電漿尾場加速器（LWFA/LPA）所產生的電子束，能在Undulator中進入指數增益（exponential-gain）自由電子雷射（FEL）工作區域，成功產生 27 nm 極紫外相干輻射，突破過去僅停留在自發輻射（spontaneous emission）的限制 。加速與束流品質使用 200 TW 等級雷射，在毫米尺度電漿中實現 >100 GV/m 的超高加速梯度，產生能量約 490 MeV 的電子束。電子束具有 ~0.5% 能量散佈、~30 pC 電荷、~0.2 mrad 發散角，

並透過永久磁鐵與電磁四極磁鐵組成的傳輸系統，有效抑制發散並維持波蕩器內的小束斑。FEL 設計與操作條件系統採用 三段Udulator（總長 4.5 m），週期 25 mm、K ≈ 1.41，對應共振波長約 27 nm。估算 FEL 參數 $\rho \approx 5\times10^{-3}$，理想增益長度約 0.23 m，實驗條件足以支撐指數增益放大。關鍵實驗證據透過「軌道擾動（orbit kick）」方法，在不同波蕩器段之間刻意破壞電子–光場耦合，直接量測輻射能量沿波蕩器長度的變化，清楚驗證 第三段波蕩器中約 100 倍的功率增益，確認系統確實進入指數增益區域。輸出輻射特性輻射中心波長 27 nm，單發最高光子數約 10^{10}，最大輻射能量約 150 nJ。雙縫干涉實驗顯示具備良好橫向相干性，符合 FEL 的基本判據。意義與前景此成果是 LPA-FEL 的關鍵概念驗證（proof-of-principle），顯示未來有機會發展 10 公尺等級、低成本、實驗室尺度的極紫外／軟 X 光 FEL

[Ref.] Nature **595**, 516-520 (2021), https://doi.org/10.1038/s41586-021-03678-x

FEL driven by a compact laser plasma accelerator (seeded FEL, 276 nm)

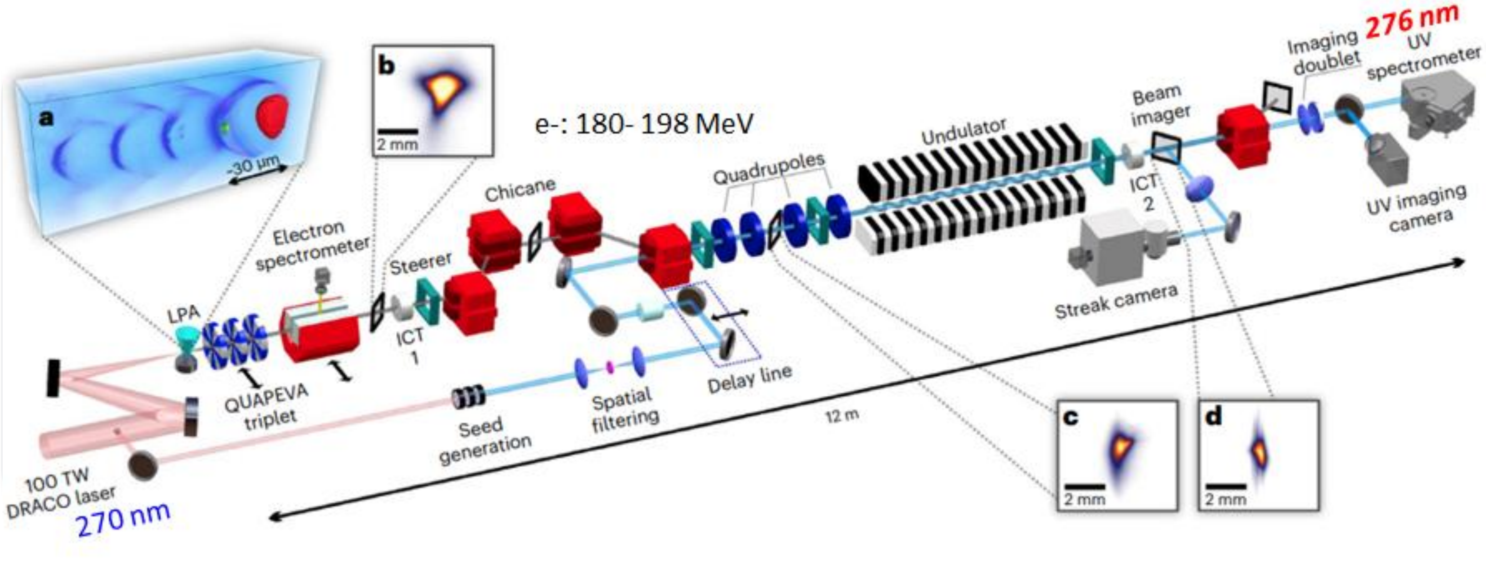

電子束來源與特性:使用 100 TW 等級 DRACO 雷射，在毫米尺度電漿中產生電子束。電子能量集中於 180–198 MeV（~188 MeV），束長原本為飛秒等級，經 chicane（R56≈−1.8 mm）拉長至約皮秒，以配合種子光與 FEL 交互作用。LPA 束流具有高峰值電流，但仍存在較大的能量散佈與 shot-to-shot 抖動，是實驗設計需克服的關鍵挑戰。種子式 FEL 架構外部種子光由主雷射分出並進行倍頻產生，中心波長約 269–270 nm，再經色散元件刻意拉長至約 1 ps，使種子光具有時間-波長 chirp。電子束與種子光在波盪器內僅於特定縱向位置滿足共振條件，啟動 FEL 能量交換。關鍵物理機制：紅移與可調波長由於電子束能量 chirp 與波盪器色散效應，初始由種子光引發的微束團調制在傳播中被拉伸，導致 FEL 輻射波長相對種子光紅移。藉由調整種子光與電子束的相對延遲，可連續控制 FEL 輻射波長（約 270–276 nm）。實驗證據與成果實驗量測顯示：FEL 輻射能量對電子束電荷呈平方關係，符合相干放大特徵輻射頻譜中出現穩定干涉條紋，證實種子光與 FEL 輻射之間的相位鎖定與縱向相干性輻射波長穩定且可預測，明顯優於 SASE 模式整體影響與前景此成果證明 LPA-driven seeded FEL 在 XUV 波段具可行性與可控制性，為未來 10–50 m 等級、低成本、實驗室型 FEL 光源鋪路

[Ref.] Nature Photonics **17**, 150-156 (2023), https://doi.org/10.1038/s41566-022-01104-w

Injector system in MAX-IV

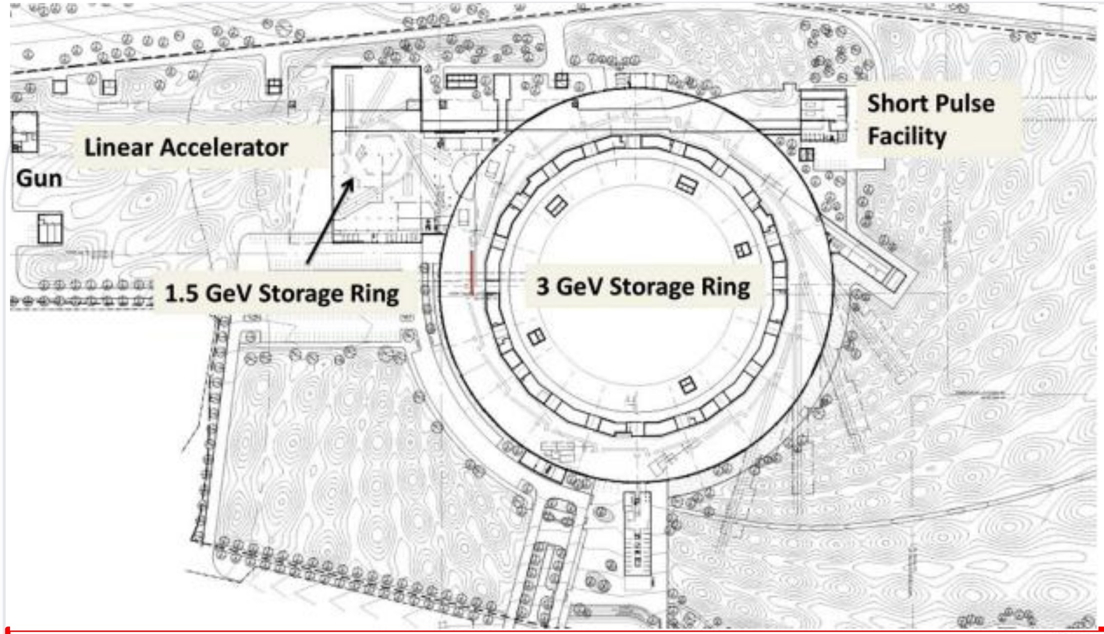

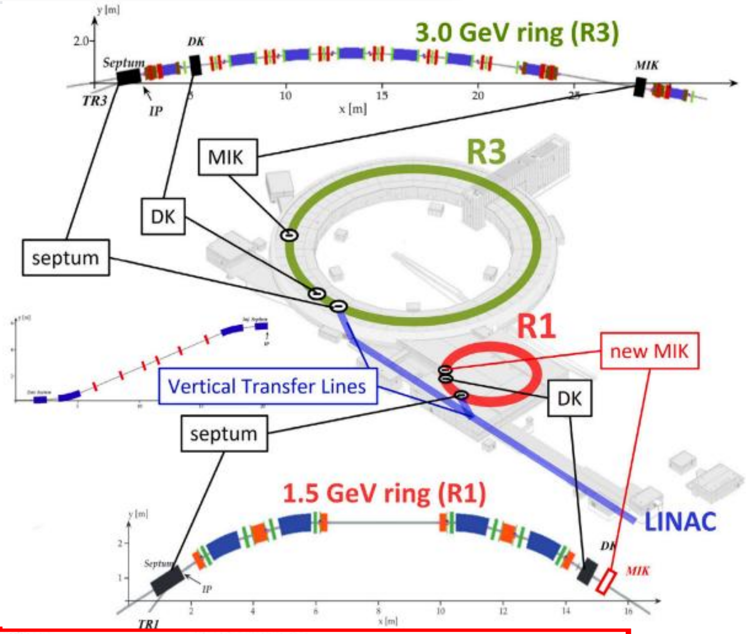

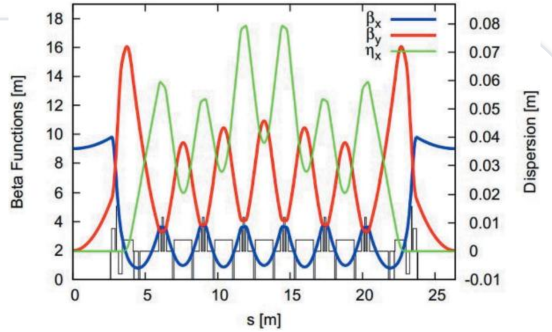

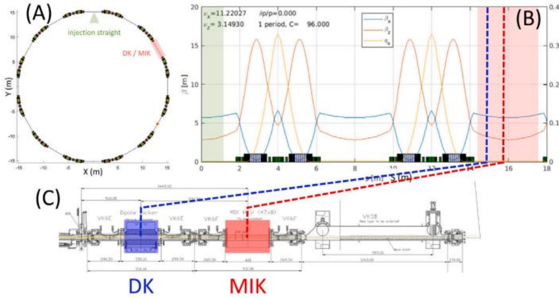

■LINAC Injector

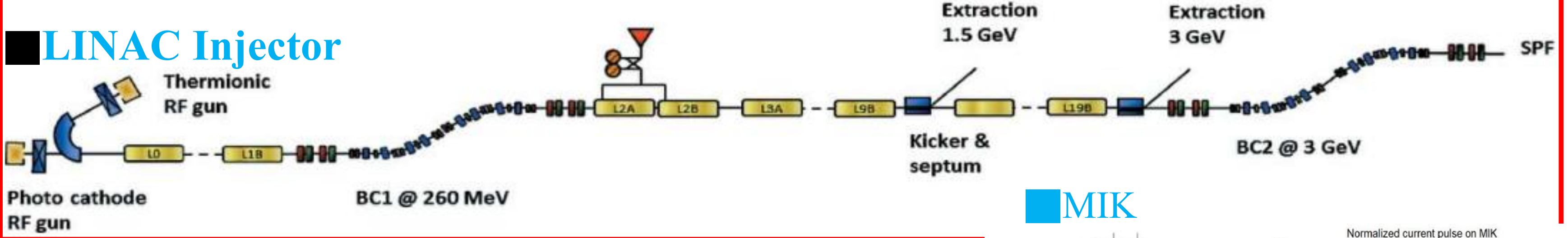

■MIK

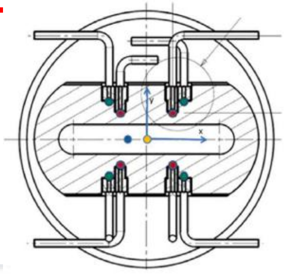

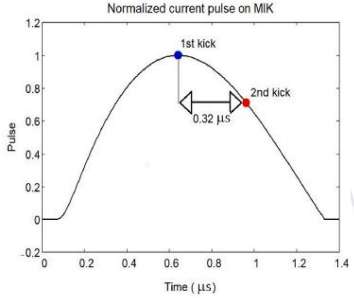

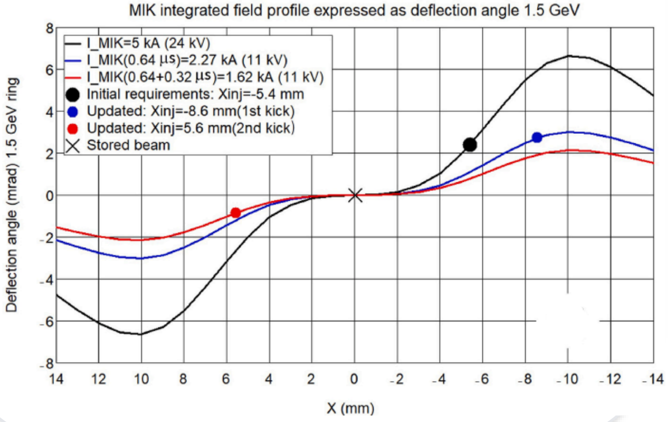

The Plasma Injector System for PETRA-IV

Enabling laser plasma accelerators (LPAs) for top applications

- Builds upon successful LPA development at DESY (LUX) for enhanced beam quality, reliability and performance (24/7).
- Active feedback with AI control for enhanced stability (KALDERA).
- Laser guiding technologies for efficient 6 GeV energy gain (HOFI).
- State-of-the-art computing capabilities for precise modeling and advanced machine learning optimization.
- Novel conceptual beamline, enabling per-mille levels of energy bandwidth and stability.

plasma injector schematic

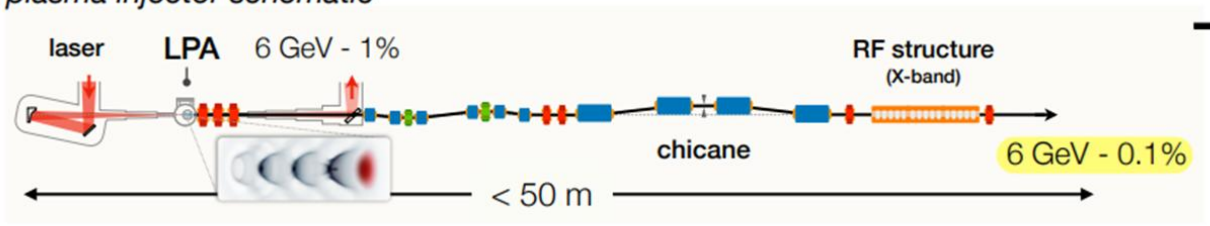

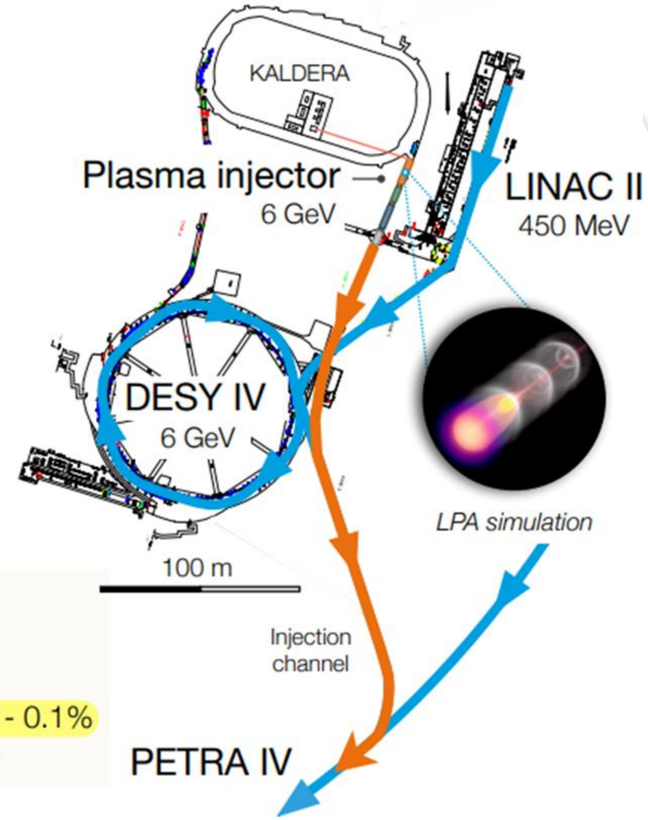

Laser Plasma Accelerator (LPA)

- **Drive Laser (Ti:Sa | λ_0=800 nm):** Peak power: ~350 TW, energy: ~20 J.
- **Plasma source (~20 cm):** Controlled injection (LUX). Efficient laser guiding (HOFI).
- **Bayesian optimization:** maximizes the beam spectral density at 6 GeV and minimizes the laser energy.

Energy Compression Beamline (ECB)

- **Quad triplet:** Beam capturing
- **Chromatic chicane:** pre-stretcher + chromaticity correction (horizontal plane)
- **Main chicane:** beam length decompression
- **X-band structure:** energy compression and stabilization

PETRA-IV未來將以 DES（LUX）多年成功的雷射電漿加速器（LPA）研發為基礎，目標是將 LPA 從實驗室示範推進到可長時間穩定運轉（24/7）、具備高束流品質、高可靠度與高性能的實用加速器，以支援同步輻射光源、FEL 與高能物理等前沿應用。束流穩定性的核心突破透過主動回饋系統結合人工智慧（AI）控制（KALDERA），即時修正雷射與電漿交互作用中的波動，大幅提升電子束能量、能散與指向穩定性，解決 LPA 長期被視為最大瓶頸的 shot-to-shot 抖動問題。高效率雷射導引與能量提升採用先進的雷射導引技術（HOFI），在約 20 公分尺度的電漿中實現單段 6 GeV 能量增益，顯著降低對雷射能量與系統長度的需求，使整體加速器保持高度緊湊。

https://accelconf.web.cern.ch/fls2023/talks/mo4b2_talk.pdf

Storage ring vs Linac FEL：物理條件與研發定位差異

Storage ring（TPS）

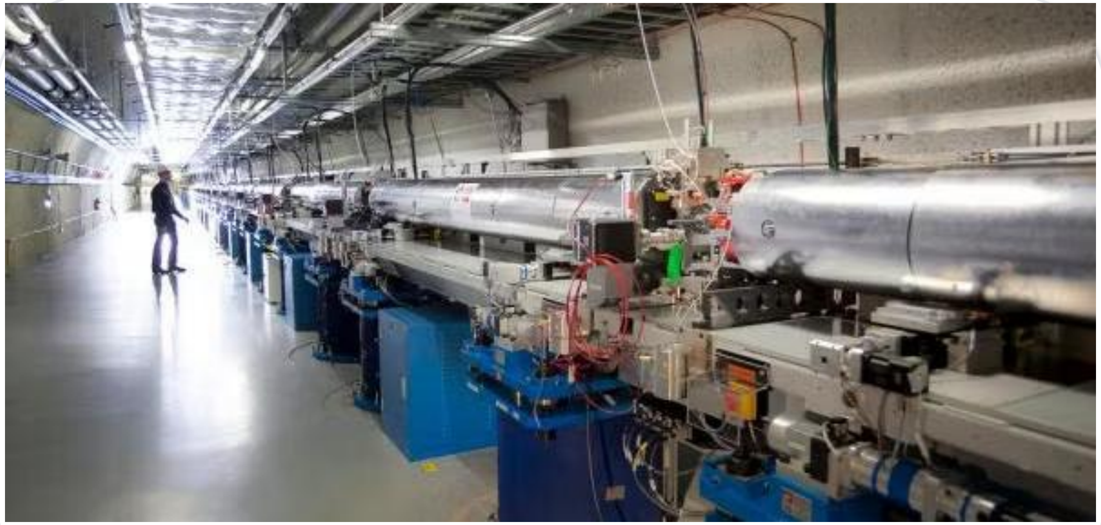

Linac FEL（LCLS）

快速比較

面向	Storage ring	Linac FEL
峰值電流 / 單次通過增益	受限（低增益路線）	可達高峰值電流 → 高增益/飽和
時間相干性（原生）	需 seeded / enhancement 才能顯著提升	SASE 已可達高功率；seeded/self-seeding 更佳
重複率 / 穩定度	高重複率、穩態、長時間統計優勢	脈衝式；可很高但系統複雜
束流模式	循環、多束團、fill pattern 可設計	單束團/少束團為主
研發定位	相干增	使用者光源（X-ray FEL）
關鍵瓶頸	阻抗→微波不穩定性、能量散、微團聚保留	壓縮、jitter、CSR/LSC 等

結論：TPS-II 的正確目標是「低增益相干增強＋縱向穩定化」，而非直接對標高增益 X-ray FEL

Comparison between Storage Ring and FEL

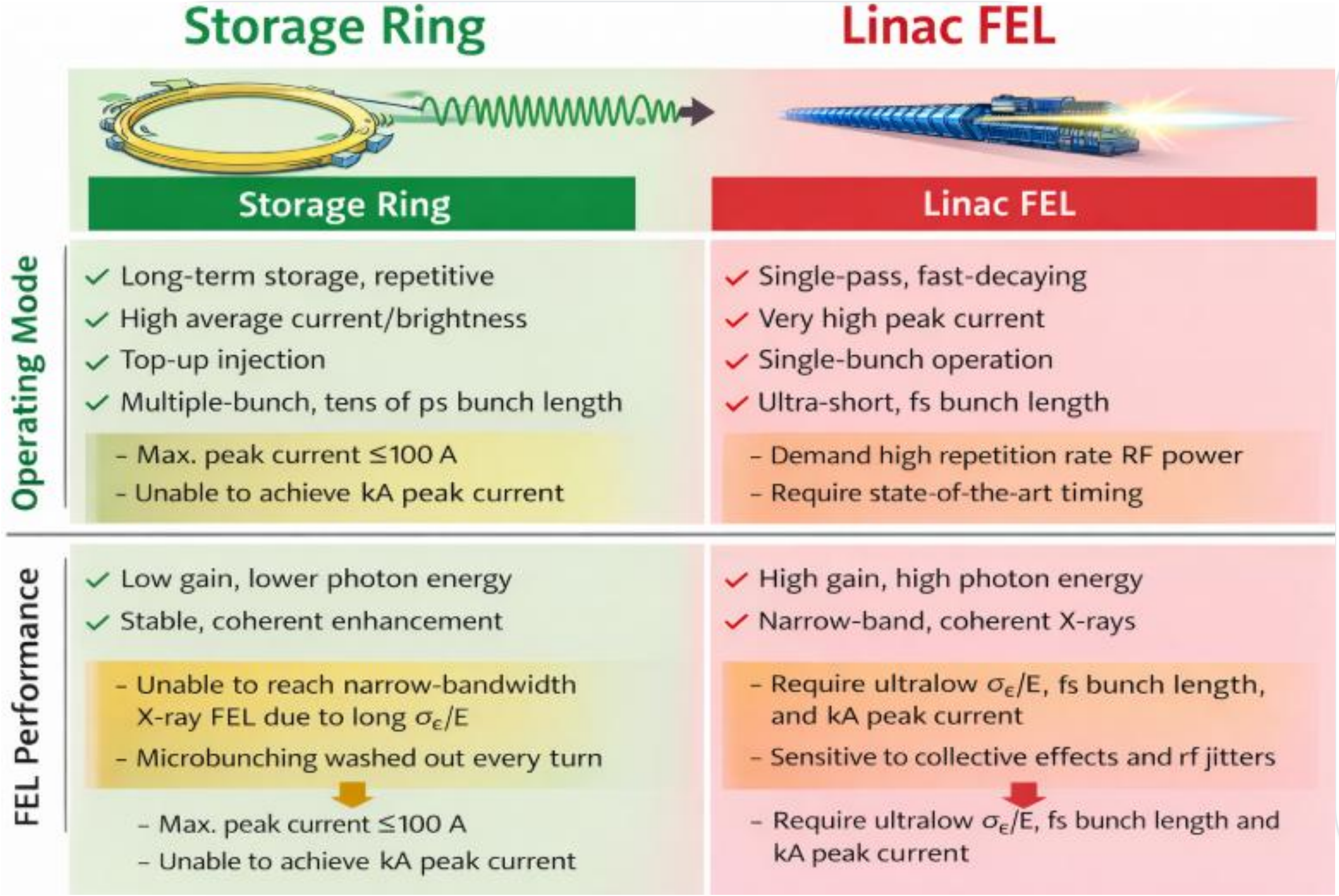

EUV high power source (~a few tens kW)

D. Ratner and W. Chao, PRL 205, 154801 (2010).
A. Chao et al., Proc. of IPAC2016, Busan, Korea (2016) pp. 1048-1053.

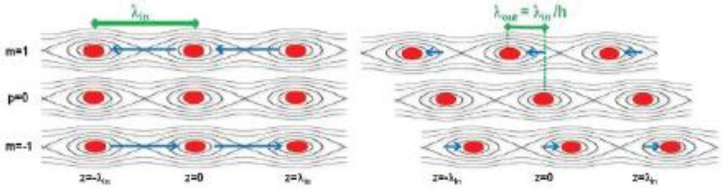

This original scheme builds micro-buckets in usual RF buckets by introducing high power laser interaction through undulator. It looks challenging to access EUV (shorter) wavelength range.

Staggered microbucket SSMB

SR-based PEHG FEL for EUV lithography

C. Feng et al., "Storage ring based PEHG FEL for EUV lithography @2016 OSA.
A. Chao et al., Proc. of IPAC2016, Busan, Korea (2016) pp. 1048-1053.

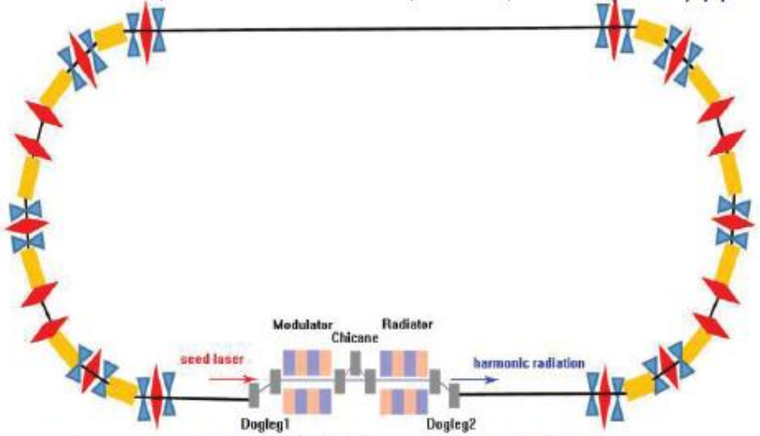

Reversible SSMB with PEHG

By using a phase-merging enhanced harmonic generation (PEHG), sustainable HHG generation has been investigated. It looks challenging to assure long term stable operation by suppressing electron beam heating.

■原始SSMB構想
出處：Ratner & Chao, PRL 2010；IPAC 2016
核心想法：在原本 RF bucket（毫米～公分尺度）裡面，用高功率雷射＋undulator建立多個雷射尺度的micro-buckets→ 每一個 micro-bucket 都是相位鎖定的微束團, 也就是：不是縮短整個bunch，而是在 RF bucket 裡面鋪很多小桶子.圖中看到的就是：外層：RF bucket 的縱向相空間內層：由雷射產生的多個穩定 micro-buckets（staggered）

■核心問題：電子束加熱（beam heating）
PEHG / FEL 類機制在儲存環中會：
•增加能散, 增加縱向與橫向 emittance,
•破壞原本的平衡態. 在 linac FEL：
•用一次就丟 → 沒問題
在儲存環：
•每一圈都在加熱
•最後：能散爆掉, 微束團失效,光源不穩定
👉「**長期穩定運轉」成為最大挑戰**